ARTICLE

Small noncoding vault RNA modulates synapse formation by amplifying MAPK signaling

Shuji Wakatsuki[1], Yoko Takahashi[1], Megumi Shibata[1], Naoki Adachi[2,3], Tadahiro Numakawa[2,4], Hiroshi Kunugi[2], and Toshiyuki Araki[1]

The small noncoding vault RNA (vtRNA) is a component of the vault complex, a ribonucleoprotein complex found in most eukaryotes. Emerging evidence suggests that vtRNAs may be involved in the regulation of a variety of cellular functions when unassociated with the vault complex. Here, we demonstrate a novel role for vtRNA in synaptogenesis. Using an in vitro synapse formation model, we show that murine vtRNA (mvtRNA) promotes synapse formation by modulating the MAPK signaling pathway. mvtRNA is transported to the distal region of neurites as part of the vault complex. Interestingly, mvtRNA is released from the vault complex in the neurite by a mitotic kinase Aurora-A–dependent phosphorylation of MVP, a major protein component of the vault complex. mvtRNA binds to and activates MEK1 and thereby enhances MEK1-mediated ERK activation in neurites. These results suggest the existence of a regulatory mechanism of the MAPK signaling pathway by vtRNAs as a new molecular basis for synapse formation.

Introduction

The establishment of axon/dendrite polarity is a critical step in neuronal differentiation (Barnes and Polleux, 2009; Yogev and Shen, 2017). Neurodevelopmental disorders, including autism spectrum disorders, are characterized at cellular levels by abnormal establishment of neuronal connectivity during development (Gilbert and Man, 2017; Mohammad-Rezazadeh et al., 2016). Subcellular signaling, involving protein kinases, plays a significant role in the establishment and regulation of neuronal connectivity at synapses. Among such kinases, the MAPK signaling pathway leading to the activation of extracellular signal-regulated kinase 1 and 2 (ERK1 and ERK2) plays a key role in regulating local protein synthesis in dendrites, formation and stabilization of dendritic spines, and synaptic plasticity in the brain (Sweatt, 2004; Thomas and Huganir, 2004). Unfortunately, the precise molecular mechanism for these regulations remains elusive.

Noncoding RNAs (ncRNAs) function at the RNA level and are not translated into proteins. Roles of ncRNAs were first characterized in protein synthesis as ribosomes or transfer RNAs, and subsequently a number of additional functions have been identified, including transcription, translation, RNA processing, and chromatin remodeling, and they also contribute to protein stability and localization (Amaral et al., 2008; Gebetsberger and Polacek, 2013; Hüttenhofer et al., 2005; Sabin et al., 2013; Tuck

and Tollervey, 2011). Small noncoding vault RNAs (vtRNAs) have been described as a component of the vault complex, a hollow, barrel-shaped ribonucleoprotein complex found in most eukaryotes (Kedersha and Rome, 1986; Stadler et al., 2009). In addition to the vtRNAs, the vault complex consists of multiple copies of three protein species: the major vault protein (MVP), the vault poly(ADP-ribose)-polymerase, and telomerase-associated protein 1 (Berger et al., 2009). The number of vtRNA paralogs differs among species: humans express four (vtRNA1-1, vtRNA1-2, vtRNA1-3, and vtRNA2-1), while mice express only one. Furthermore, recent reports have suggested that vtRNA may function to regulate cellular pathophysiology. Overexpression of vtRNA1-1 was shown to be protective against apoptosis in a cellular model of Epstein–Barr virus infection, to support influenza virus replication via protein kinase R inactivation, and to act as a regulator of autophagy function (Horos et al., 2019; Li et al., 2015; Nandy et al., 2009). Importantly, dysregulation of vtRNAs has been also linked with brain cancers, intellectual disability, and neurodegeneration (Barry et al., 2014; Hussain and Bashir, 2015; Miñones-Moyano et al., 2013). Thus, it has been suggested that the function of vtRNAs might not be limited to simply maintaining the structure of the vault complex. Despite the increasing research on vtRNAs, little is known about their physiological functions.

[1]Department of Peripheral Nervous System Research, National Institute of Neuroscience, National Center of Neurology and Psychiatry, Tokyo, Japan;   [2]Department of Mental Disorder Research, National Institute of Neuroscience, National Center of Neurology and Psychiatry, Tokyo, Japan;   [3]Department of Biomedical Chemistry, School of Science and Technology, Kwansei Gakuin University, Hyogo, Japan;   [4]Department of Cell Modulation, Institute of Molecular Embryology and Genetics, Kumamoto University, Kumamoto, Japan.

Correspondence to Shuji Wakatsuki: swaka@ncnp.go.jp;   Toshiyuki Araki: taraki@ncnp.go.jp.

Here, we show a novel role for vtRNA in synaptogenesis. Using a model of synaptogenesis in vitro, we demonstrate that murine vtRNA (mvtRNA) up-regulates synaptogenesis by activating the MAPK signaling pathway. mvtRNA is transported in neurites as a part of the vault complex. Interestingly, mvtRNA is released from the vault complex in neurites, which is triggered by MVP phosphorylation mediated by a mitotic kinase, Aurora-A. mvtRNA binds to and activates mitogen-activated protein kinase kinase 1 (MEK1) and thereby enhances MEK1-mediated ERK activation. These results identify the regulatory mechanism of MAPK signaling pathway through mvtRNA as a novel molecular basis for synaptogenesis. This is the first characterization of mvtRNA, a putative riboregulator of synaptogenesis.

Results

Aurora-A interacts with MVP in postmitotic neurons

Previous studies have reported that the mitotic kinase Aurora-A, known as a kinase involved in cellular mitotic processes, plays a role in regulation of the morphological differentiation of postmitotic neurons, such as neurite outgrowth and neuronal polarity formation (Khazaei and Püschel, 2009; Mori et al., 2009; Pollarolo et al., 2011). We found by screening commercially available small-molecule kinase inhibitor libraries that application of an Aurora-A inhibitor in cultured hippocampal neurons disrupted neuronal polarity. This result was subsequently confirmed by using specific shRNAs for Aurora-A (data not shown). These findings motivated us to search for the downstream effectors involved in this pathway. To identify substrates for Aurora-A kinase activity, we first set up a coimmunoprecipitation experiment to search for proteins that associate with Aurora-A. For this purpose, cultured cortical neurons were infected with adenovirus expressing HA-tagged Aurora-A, and then cell lysates were used for the immunoprecipitation assay with anti-HA antibody. The immunoprecipitates of anti-HA antibody were analyzed by SDS-PAGE with silver staining. The specific band at 100 kD was analyzed by mass spectrometry (Fig. 1 A, open arrowhead). The masses of the trypsin-digested peptides were queried against the Swiss-Prot database, which returned a match identifying p100 as the murine MVP (Fig. 1 B). MVP is a major structural protein of the vault complex, contributing 70% to the complex mass, and self-assembles to form a vault-like structure in vivo (Berger et al., 2009; Kickhoefer et al., 1996; van Zon et al., 2003a). To examine whether MVP is a substrate for Aurora-A kinase activity, we overexpressed WT or the mutant forms of Aurora-A in murine neuroblastoma Neuro-2a cells (Fig. S1) and cultured cortical neurons (Fig. 1, C–E). We found by immunoprecipitation experiments using lysates of these cells that both WT and kinase-dead mutant (K153R) forms of Aurora-A can similarly associate with MVP (Figs. 1 D and S1). We also found that the overexpression of Aurora-A K153R inhibits MVP phosphorylation, while overexpression of either WT or a constitutively active (T288D) form of Aurora-A enhanced MVP phosphorylation on serine residues (Fig. 1, D and E; and Fig. S1). Collectively, these results indicate that Aurora-A associates with and phosphorylates MVP.
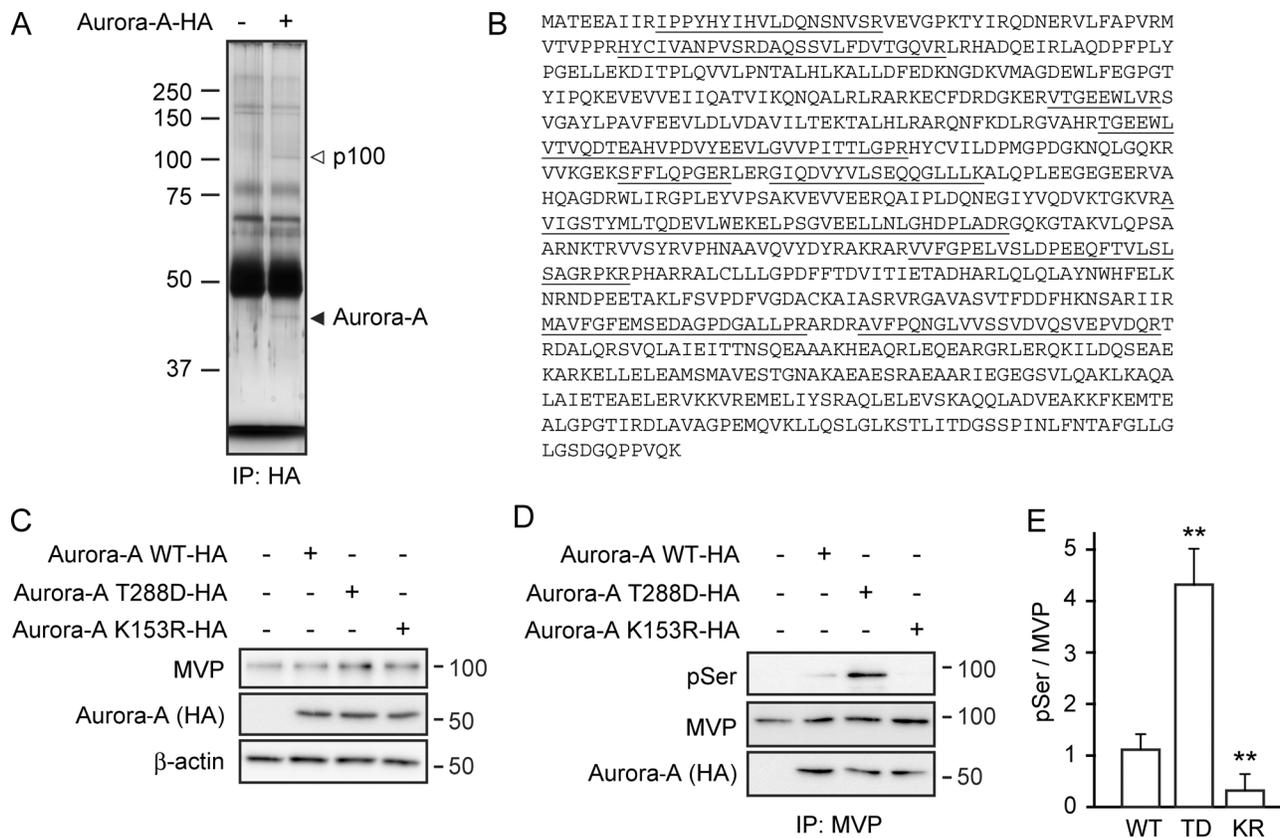
Aurora-A interacts with MVP in the postsynaptic region

MVP has been shown to be required for brain development in invertebrate species (Blaker-Lee et al., 2012; Pan et al., 2013; Paspalas et al., 2009). To investigate changes in molecular interaction between MVP and Aurora-A in brain development, we first examined developmental changes in the expression of MVP and Aurora-A protein in mouse brains (Fig. 2, A–C). We found that the protein level of MVP became significantly higher in a mature brain (postnatal day 35 [P35]) compared with that in a developing brain (P14) and remained high through adulthood (>P70). In contrast, the expression level of Aurora-A did not change (Fig. 2, A and C). To examine the developmental change of the MVP–Aurora-A association, we performed coimmunoprecipitation experiments using an antibody against Aurora-A from brain lysates. The interaction between MVP and Aurora-A became stronger in the mature brain compared with that in the developing brain (Fig. 2, B and C). These results suggest that the interaction between MVP and Aurora-A is developmentally regulated.

Since previous studies have shown that Aurora-A is present at synapses in neurons (Huang et al., 2002; Richter and Sonenberg, 2005), we hypothesized that Aurora-A might associate with MVP at synapses. To examine this possibility, we first examined the localization of Aurora-A and MVP at synaptic regions. For this purpose, we performed sequential centrifugation to fractionated extracts of adult mouse brain (Fig. 2 D). We found by immunoblot analysis of separated fractions that Aurora-A and MVP are more strongly detected in the postsynaptic density (PSD) fractions than in the synaptosome fractions. To examine whether Aurora-A associates with MVP at synapses, we performed coimmunoprecipitation experiments using the detergent-extracted PSD fractions to demonstrate the interaction between Aurora-A and MVP (Fig. 2, E and F). We observed a specific interaction between Aurora-A and MVP in immunoprecipitates using antibodies against Aurora-A and MVP, but not control IgG. We also found MVP phosphorylation on serine residues in the immunoprecipitates. These results suggest that Aurora-A associates with and phosphorylates MVP in the postsynaptic region. To further define the association of MVP with Aurora-A, we examined immunocytochemical colocalization of MVP and Aurora-A in cultured cortical neurons (Fig. 2 G). We found some of the structures immunostained for both MVP and Aurora-A were also positive for PSD-95, suggesting that MVP and Aurora-A are located in the PSD95-positive postsynaptic terminals of neurons. Taken together, our findings demonstrate MVP association with Aurora-A at the postsynaptic regions.

Aurora-A together with MVP enhances synapse formation and activity by the activation of ERK signaling

Previous reports suggested that MAPK and AKT signaling pathways are the major downstream mechanism for Aurora-A kinase activity (Carmena and Earnshaw, 2003; Nikonova et al., 2013; van Zon et al., 2003b). To examine whether either of these two pathways is activated in an Aurora-A–dependent manner, we examined the activation status of each signaling pathway in Neuro-2A cells (Fig. S2) and cultured cortical neurons (Fig. 3, A
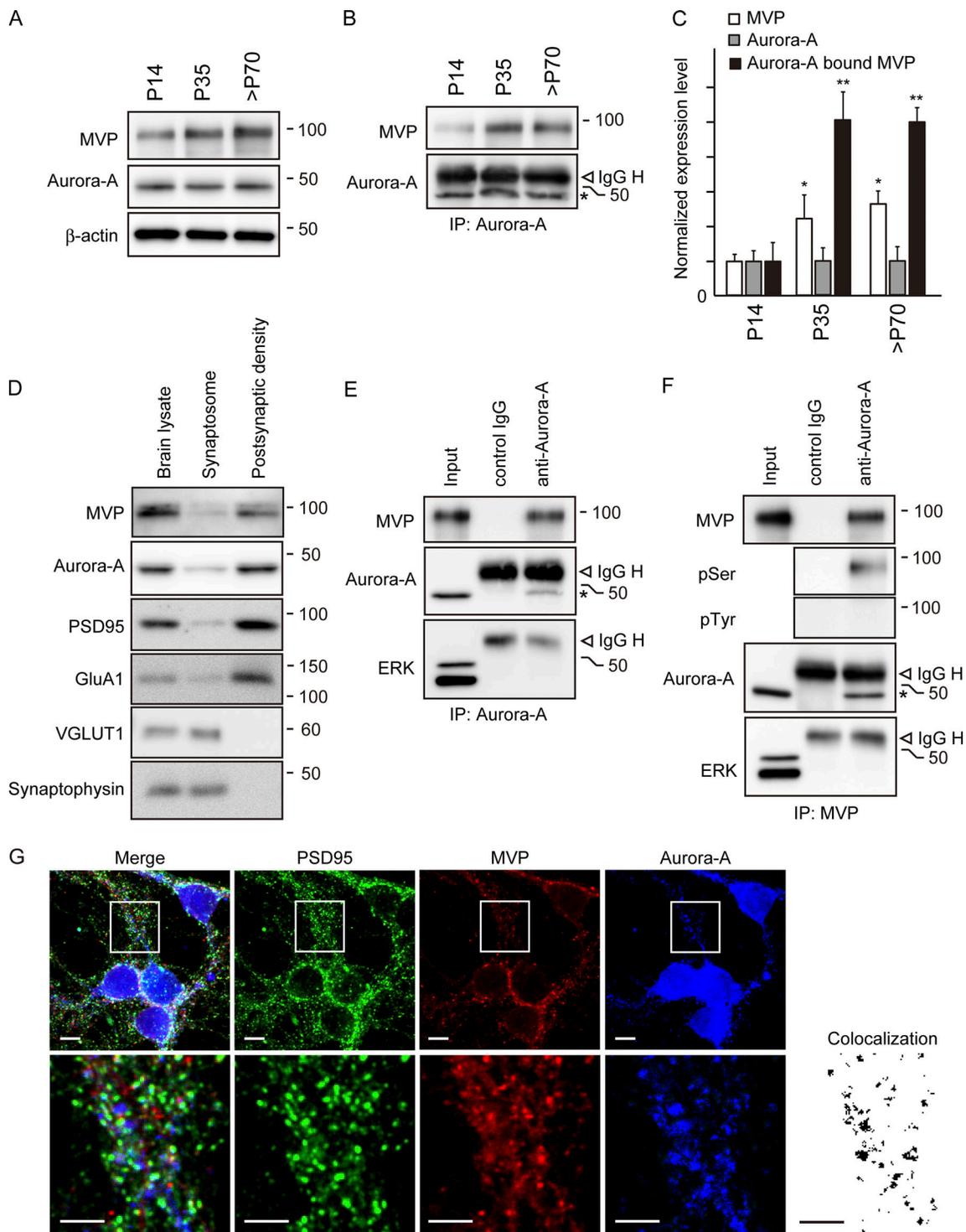
Figure 1. **Aurora-A interacts with MVP in postmitotic neurons. (A and B)** Identification of MVP as a binding protein for Aurora-A kinase in postmitotic neurons. Lysates were prepared from cultured cortical neurons overexpressing HA-tagged Aurora-A. Representative immunoprecipitation using an anti-HA antibody analyzed by SDS-PAGE with silver staining (A). The specific band at 100 kD (open arrowhead) was analyzed by liquid chromatograph–mass spectrometry (LC-MS/MS), and results were searched against Swiss-Prot. Mass-predicted peptides exhibited a 31.4% (underlined) match to murine MVP (B). Open arrowhead and filled arrowhead indicate a band of MVP and HA-tagged Aurora-A, respectively. **(C–E)** MVP is associated with and phosphorylated by Aurora-A in cultured cortical neurons. Lysates were prepared from cultured cortical neurons infected with adenovirus expressing HA-tagged WT Aurora-A, mutant forms of Aurora-A T288D, or K153R. Representative immunoblots (C) and immunoprecipitations using an antibody against MVP (D) analyzed by immunoblotting with indicated antibodies. β-Actin serves as a loading control. Quantified expression levels for phosphorylated MVP normalized to total MVP relative to the mock-transfected control (mean ± SEM, $n = 5$; E). Significant differences from the control (**, $P < 0.01$) were determined by a one-way ANOVA with Tukey's post hoc test. pSer, phospho-serine; IP, immunoprecipitation; TD, T288D; KR, K153R.

and B) overexpressing either WT Aurora-A or its mutants. We found dramatic enhancement of ERK phosphorylation by overexpressing either WT Aurora-A or T288D, but not K153R together with MVP in cultured cortical neurons (Fig. 3, A and B). This is similar to what was observed using Neuro-2A cells (Fig. S2). In contrast, the phosphorylation status of AKT was unaffected by the overexpression of either WT Aurora-A or its mutants. Importantly, overexpression of either WT Aurora-A or its T288D mutant together with MVP dramatically enhanced the phosphorylation of ERK, but not AKT (Fig. 3, A and B; and Fig. S2). These results suggest that Aurora-A in concert with MVP enhances ERK signaling.

Since the MAPK signaling pathway has key roles in regulating local protein synthesis in dendrites, dendritic spine formation, and synaptic function (Sweatt, 2004; Thomas and Huganir, 2004), we hypothesized that the interaction of Aurora-A with MVP at synapses leads to enhancement of ERK activity to increase synapse formation. To know whether the Aurora-A and MVP-dependent ERK activation affects synaptic activity, we first examined expression of presynaptic (Synapsin

I and Synaptophysin) and postsynaptic (PSD95 and an AMPA-type glutamate receptor, GluA1) marker proteins in cultured mouse cortical neurons overexpressing Aurora-A and MVP. As expected, we found by immunoblot analysis using lysates from these cells that overexpression of either WT or T288D Aurora-A, but not K153R mutant, together with MVP increases the expression of synaptic marker proteins (Fig. 3, A, C, and D). We also found an increased number of PSD95 and Synapsin I double-positive puncta in neurons expressing either WT or T288D Aurora-A, but not K153R mutant, together with MVP (Fig. 3, E and F). These results suggest that Aurora-A– and MVP-dependent ERK activation increases the synapse number in neurons.

The activity-dependent uptake of the FM dye into synaptic vesicles allows resolution of individual synaptic puncta and has also proven useful in the visualization of active synapses (Cochilla et al., 1999). To determine whether the increased number of synapses formed by Aurora-A– and MVP-dependent ERK activation leads to increased synaptic activity, we exposed neurons overexpressing WT or mutant forms of Aurora-A

Figure 2. **Aurora-A interacts with MVP at the PSD. (A–C)** Expression of MVP and Aurora-A proteins in brains during development. Cell lysates were prepared from brains at the indicated time point. Representative immunoblots (A) and immunoprecipitations (B) using an antibody against Aurora-A analyzed by immunoblotting. β-Actin serves as a loading control for immunoblots. **(C)** Quantified expression levels of MVP and Aurora-A normalized to β-actin at the indicated time points relative to the expression levels at P14 (mean ± SEM, $n = 3$ animals for each time point). For immunoprecipitation, quantified levels of MVP protein normalized to Aurora-A at the indicated time points are shown relative to the level at P14 (mean ± SEM, $n = 3$ animals for each time point). Significant differences from the P14 levels (*, $P < 0.05$; **, $P < 0.01$) were determined by one-way ANOVA with Tukey's post hoc test. **(D)** Aurora-A and MVP are present in the PSD. Synaptosome and PSD fractions were prepared from adult brain lysate. Brain lysate, synaptosome, and detergent-extracted PSD fractions were analyzed by immunoblot using the indicated antibodies. Representative immunoblots are shown. **(E and F)** The Aurora-A–MVP complex is detected in the PSD. The interaction between Aurora-A and MVP was assessed in coimmunoprecipitation experiments using antibodies against Aurora-A (E) and MVP (F) in the detergent-extracted PSD fractions prepared from adult brain lysate. Representative immunoprecipitations analyzed by immunoblotting using the indicated antibodies are shown. Asterisk indicates Aurora-A. pSer, phospho-serine; pTyr phospho-tyrosine; IgG H, IgG heavy chain; IP,

immunoprecipitation. **(G)** MVP colocalizes with Aurora-A at the PSD95-positive postsynaptic terminals in cultured cortical neurons. Representative photomicrographs of cultured cortical neurons immunostained MVP (red), Aurora-A (blue), and PSD95 postsynaptic terminals (green). High-power images (lower) show the boxed area from the upper image. The colocalization panel shows the triple-positive puncta extracted from the merged image (shown in black). Scale bar, 25 µm.

together with MVP to FM4-64FX, a fixable analogue of FM4-64 (Bodrikov et al., 2017; Yao et al., 2010), followed by depolarization with potassium chloride stimulation (Fig. 4, A–C). We found an increased number of Synapsin I–positive puncta colabeled with FM4-64FX in neurites overexpressing Aurora-A together with MVP than in those expressing Aurora-A or MVP alone. Mean fluorescence intensity of FM4-64FX dye per puncta relative to the control was also significantly enhanced in neurons overexpressing Aurora-A together with MVP. These results suggest that Aurora-A in concert with MVP leads to not only increased numbers of synapses but also enhanced synaptic activity. To know whether this signaling affects neuronal activity, we examined Ca^{2+} levels in neurons overexpressing MVP and Aurora-A. We observed that the glutamate-stimulated Ca^{2+} increase in cortical neurons was enhanced by overexpressing MVP alone (Fig. 4 D). In line with a modest effect on activation of ERK signaling, no significant enhancement in the glutamate-stimulated Ca^{2+} increase was observed by overexpressing Aurora-A alone. Importantly, enhancement in Ca^{2+} elevation was significantly greater in cortical neurons overexpressing Aurora-A together with MVP than in those expressing MVP alone. These results suggest that Aurora-A– and MVP-dependent ERK activation increases neuronal excitability.

To confirm the roles of Aurora-A– and MVP-dependent ERK activation in neurons, we performed RNAi-mediated down-regulation of either *aurkA* or *mvp* in cultured mouse cortical neurons (Figs. 5 and S3 A). We found that down-regulation of either *aurkA* or *mvp* decreased the expression levels of synaptic marker proteins, as well as the number of PSD95 and Synapsin I double-positive puncta (Fig. 5). We also found that overexpression of shRNA-resistant cDNA of either *aurkA* or *mvp* rescues the effects of the down-regulated expression. Taken together, these results indicate that Aurora-A in concert with MVP might enhance synapse formation through the activation of ERK signaling.

MVP has been suggested to function as a scaffold to interact with ERK and regulate its signal transduction (Berger et al., 2009; Kim et al., 2006; Kolli et al., 2004). Since ERK protein was found in the postsynaptic region (Fig. 2, E and F), it is possible to speculate that MVP is a physiological scaffold for ERK signaling. To investigate whether MVP might interact with ERK at the postsynaptic region, we performed coimmunoprecipitation experiments using the detergent-extracted PSD fractions. We found by immunoblot analysis that the interaction of MVP with ERK was not observed (Fig. 2, E and F). Tyrosine phosphorylated MVP, which has been shown to be important for its binding to ERK (Kim et al., 2006; Kolli et al., 2004), was not detected either. Although the function of MVP as a scaffold for ERK signaling in the postsynaptic region has not been proven, MVP in concert with Aurora-A does enhance synapse formation through the activation of ERK signaling, which may be the

justification for vtRNA-mediated activation of ERK signaling described later.

Small noncoding mvtRNA enhances synapse formation by the activation of ERK signaling

vtRNAs have been described as small ncRNA components of the vault complex (Kickhoefer et al., 1996; Stadler et al., 2009). Recently, vtRNAs have been reported to regulate protein function (Tuck and Tollervey, 2011). While the number of vtRNA molecular varieties vary between species, there is only one mouse vtRNA (mvtRNA; Nandy et al., 2009). Therefore, to examine the possibility that vtRNA might participate in synaptic formation, we assessed the effect of overexpression of mvtRNA on synapse formation (Fig. 6, A and B). We found that overexpression of mvtRNA using a lentivirus vector in cultured neurons increased the expression of synaptic marker proteins, ERK phosphorylation, and the number of PSD95 and Synapsin I double-positive puncta, suggesting that the overexpression of mvtRNA may enhance synapse formation. To confirm the involvement of mvtRNA on synapse formation, the mvtRNA in cultured neurons was down-regulated by transfecting chemically modified antisense oligonucleotides (ASOs), as reported previously (Fig. S3 B; Li et al., 2015). We found that mvtRNA down-regulation significantly suppressed the expression of synaptic marker proteins, ERK phosphorylation, and the number of PSD95 and Synapsin I double-positive puncta (Fig. 6, C and D). These results further suggest that mvtRNA serves as a regulator of synapse formation by modulating ERK activity.

## mvtRNA is transported alongside the vault complex

Previous reports have suggested that the vault complex acts as a scaffold for proteins involved in signal transduction (Berger et al., 2009; Kim et al., 2006; Kolli et al., 2004). To uncover whether vtRNA-dependent promotion of synapse formation requires vault complex, we employed the Twiss filter system, which allows efficient purification of neurite material for biochemical analyses. We were able to examine whether down-regulation of *mvp* expression in cultured cortical neurons affects the expression of mvtRNA in cell bodies and neurites (Fig. 7). In normal conditions, we found that the expression of mvtRNA was detected in cell bodies and neurites of cultured cortical neurons. Expression of mvtRNA was barely detectable in neurites when *mvp* expression was knocked down. We found that the down-regulation of *mvp* expression did not affect the mvtRNA expression in cell bodies. We also found that the overexpression of shRNA-resistant cDNA of *mvp* rescues the effects of the down-regulated expression (Fig. 7, A and B). Previous reports have suggested that MVP may be transported within neurites by fast transporters (Herrmann et al., 1999; Li et al., 1999). MVP has also been reported to associate with several mRNAs that are translated within dendrites, including tissue plasminogen activator and striatal-enriched tyrosine
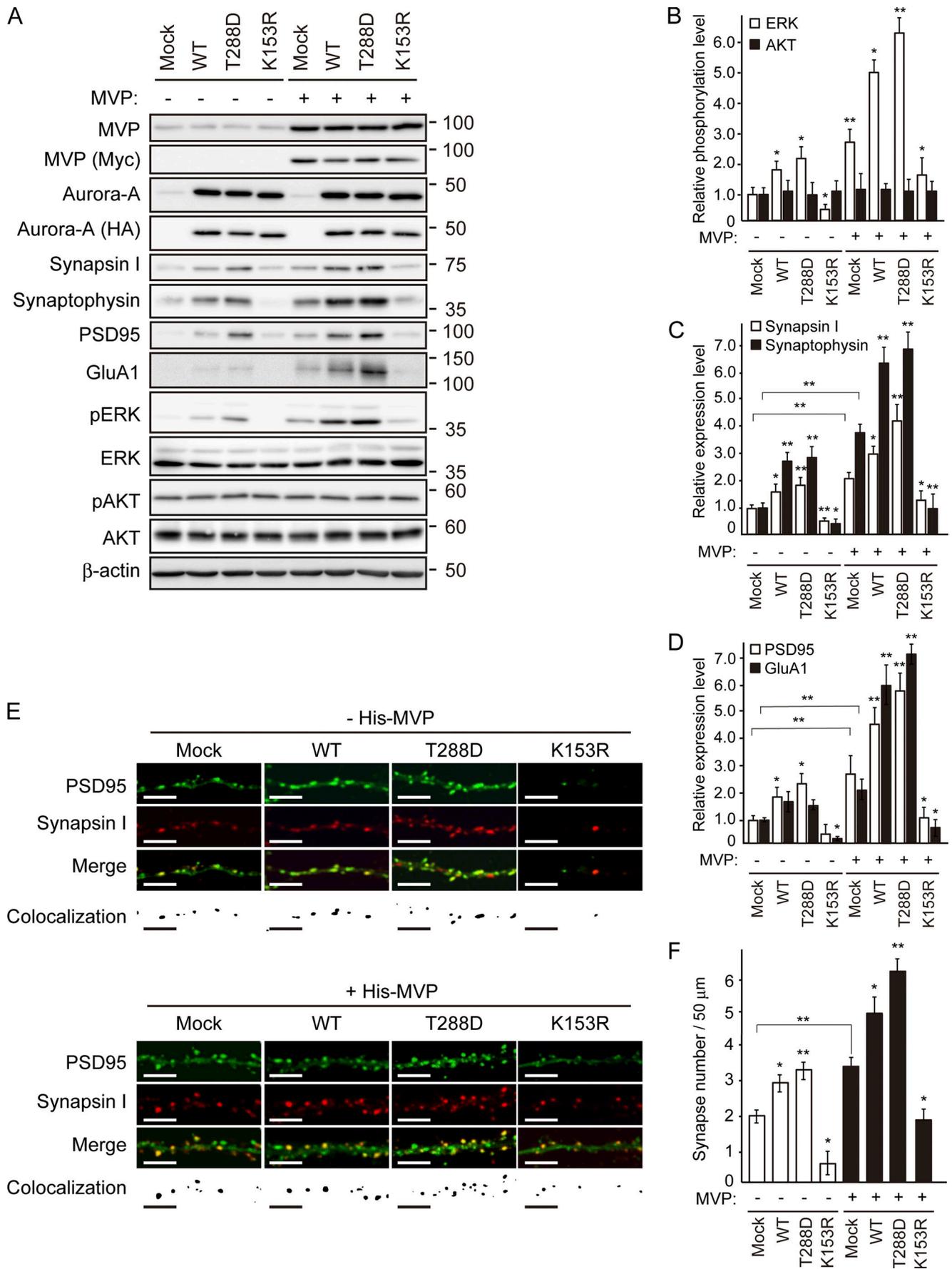
Figure 3.   **Aurora-A in concert with MVP enhances synapse formation and activity by the activation of ERK signaling. (A–F)** Aurora-A in concert with MVP enhances synapse formation through the activation of ERK signaling. Cortical neurons from murine embryonic day 14 embryos were cultured. At 5 DIV, the neurons were infected with adenovirus vectors expressing the indicated molecules. Representative immunoblots for the expression of the indicated molecules are shown in A. β-Actin serves as a loading control. Phosphorylation levels of ERK (B, calculated as phosphorylated ERK/total ERK) and expression levels of presynaptic markers Synapsin I and Synaptophysin (C) or postsynaptic markers PSD95 and GluA1 (D) normalized to β-actin relative to the value for mock-transfected control without MVP expression (mean ± SEM, n = 5). Synapse formation was assessed by double immunostaining with antibodies against PSD95 and Synapsin I. Representative photomicrographs of cultured cortical neurons infected with adenovirus for indicated molecules at 14–16 DIV (E) and the number of synapses per dendrite length (F). The colocalization panels highlight the double-positive puncta for each protein that were identified as synapses (shown in black). Scale bar, 25 µm in E. Note that cortical neurons overexpressing either WT Aurora-A or T288D, but not K153R, together with MVP display the enhancement of synapse formation. Significant differences from the control (*, $P < 0.05$; **, $P < 0.01$) were determined by one-way ANOVA with Tukey's post hoc test.

phosphatase (Paspalas et al., 2009). These previous findings and our results suggest the possibility that mvtRNA is transported alongside the vault complex. To further examine this possibility, we performed coimmunoprecipitation experiments using an antibody against MVP from neurites and revealed that the immunopurified MVP–Aurora-A complex contains the kinesin superfamily protein KIF5, but not KIF3 protein (Figs. 7 C and S4). These results suggest that mvtRNA is transported in neurites alongside the MVP–Aurora-A complex.

Previous reports have suggested that structural modifications to the vault complex may affect its function (Berger et al., 2009; Kickhoefer et al., 1998). However, the mechanism that regulates the integrity of the vault complex has not yet been described. To determine whether Aurora-A–dependent MVP phosphorylation can affect the integrity of the vault complex, we examined whether the sedimentation profile of MVP by centrifugation can be changed by Aurora-A–dependent MVP phosphorylation. For this purpose, cultured mouse cortical neurons were infected
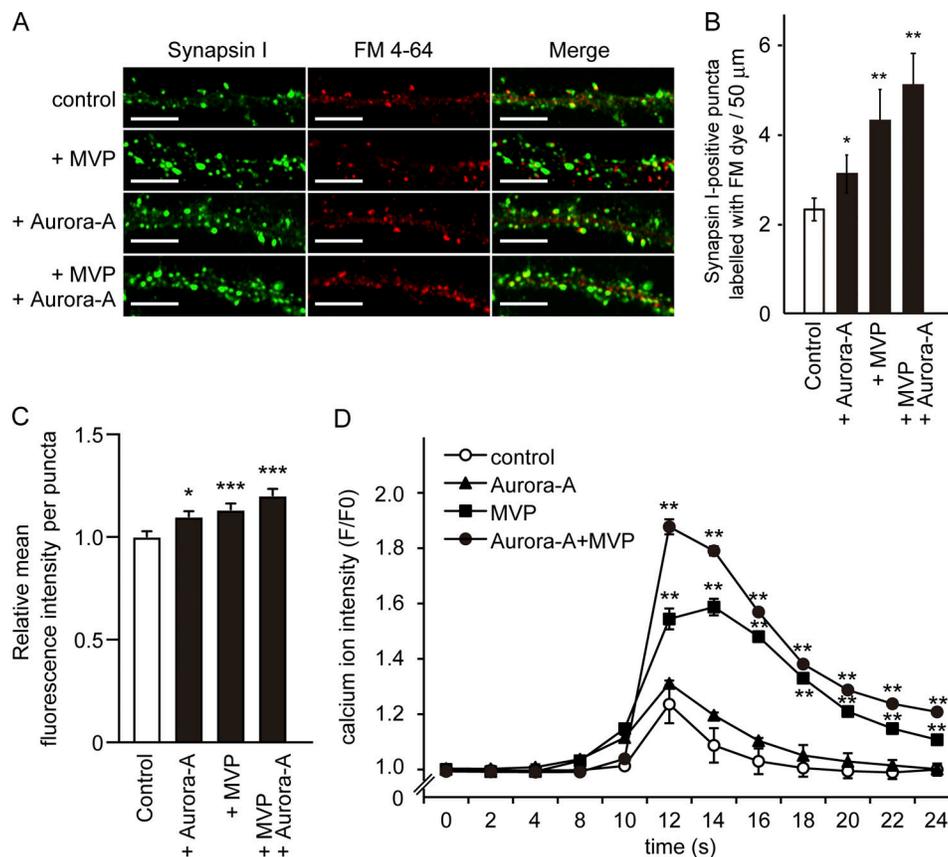

Figure 4.   **Aurora-A in concert with MVP enhances synaptic activity. (A)** Representative fluorescence images of cortical neurons infected with adenovirus for indicated molecules at 14–16 DIV and loaded with FM4-64FX followed by depolarization with potassium chloride stimulation. Scale bar, 25 µm. **(B)** The number of Synapsin I–positive puncta labeled with FM4-64FX on 50-µm dendrite. **(C)** Quantitative analysis of FM4-64FX uptake in synapses. Histograms of mean fluorescence values per Synapsin I–positive puncta relative to the control for neurons expressing the indicated genes (mean ± SEM, n = 3). The data were obtained from >300 synaptic puncta per each experimental condition. **(D)** Glutamate-triggered intracellular Ca^{2+} elevation was measured using cortical neurons overexpressing WT Aurora-A together with MVP. Note that the increase in Ca^{2+} elevation was significantly greater in cortical neurons overexpressing Aurora-A together with MVP than in those expressing MVP alone. Significant differences from the control (*, $P < 0.05$; **, $P < 0.01$; ***, $P < 0.001$) were determined by a one-way ANOVA with Tukey's post hoc test.
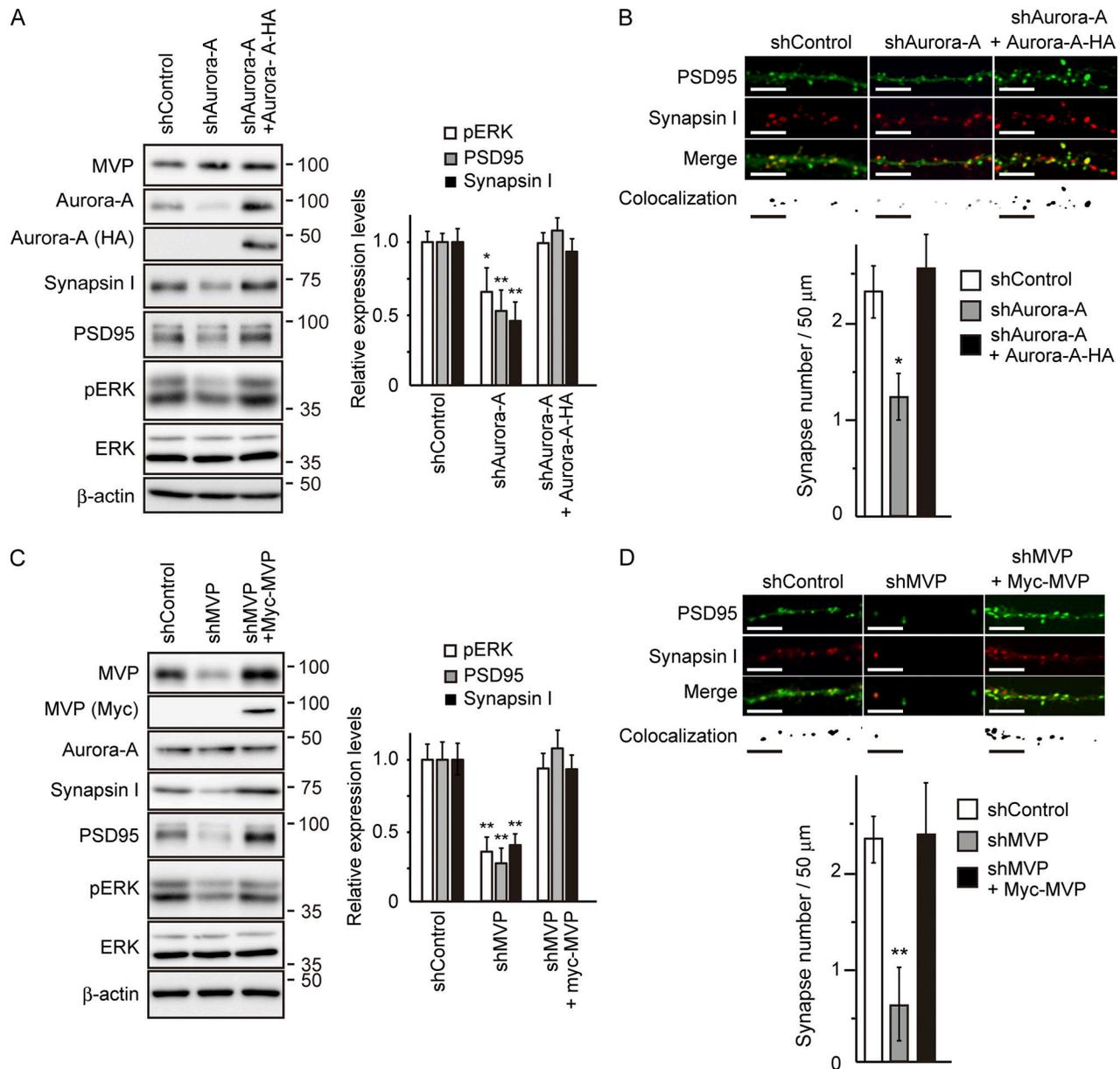
Figure 5. **Down-regulation of *aurkA* and *mvp* expression suppresses synapse formation. (A and C)** Lysates were prepared from cultured cortical neurons infected with lentivirus expressing the indicated shRNA. Representative immunoblots for the expression of the indicated molecules are shown in A and C. β-Actin serves as a loading control. Phosphorylation levels of ERK (calculated as phosphorylated ERK/total ERK) and expression levels of Synapsin I or PSD95 normalized to β-actin relative to shControl-transfected condition (mean ± SEM, n = 5) are also shown. **(B and D)** Synapse formation was assessed by double immunostaining with antibodies against PSD95 and Synapsin I. Representative photomicrographs of cultured cortical neurons infected with adenovirus for indicated molecules at 14–16 DIV, and the number of synapses per dendrite length are shown. Colocalization panels show the double-positive puncta extracted from the merged images that were identified as synapses (shown in black). Scale bar, 25 µm in E. Note that the RNAi phenotypes were rescued by coexpression of shRNA-resistant cDNA. Significant differences from control (*, $P < 0.05$; **, $P < 0.01$) were determined by a one-way ANOVA with Tukey's post hoc test.

with adenovirus expressing WT Aurora-A and its mutants, followed by examination of changes in MVP localization using fractionation of neurite cell lysates by ultracentrifugation (Fig. 7, D–F). High molecular weight particles, including the vault complex, are precipitated (P100 fraction) and separated from the soluble cytoplasmic fraction (S100 fraction). In agreement with previous reports (Kickhoefer et al., 1998; Lee et al., 2011), we found MVP exclusively in the P100 fraction in the analysis of neurites from WT cortical neurons (Fig. 7, D and E). On the other

hand, upon analysis of neurites overexpressing WT Aurora-A and Aurora-A T288D, MVP was detected in both the P100 fraction and the S100 fraction. In contrast, overexpression of Aurora-A K153R did not affect the sedimentation profile of MVP in neurites. These results suggest that the kinase activity of Aurora-A might affect the integrity of the vault complex. To know whether these Aurora-A-dependent structural changes of the vault complex affect the localization of mvtRNA as well, we examined the levels of mvtRNA expression in S100 fractions
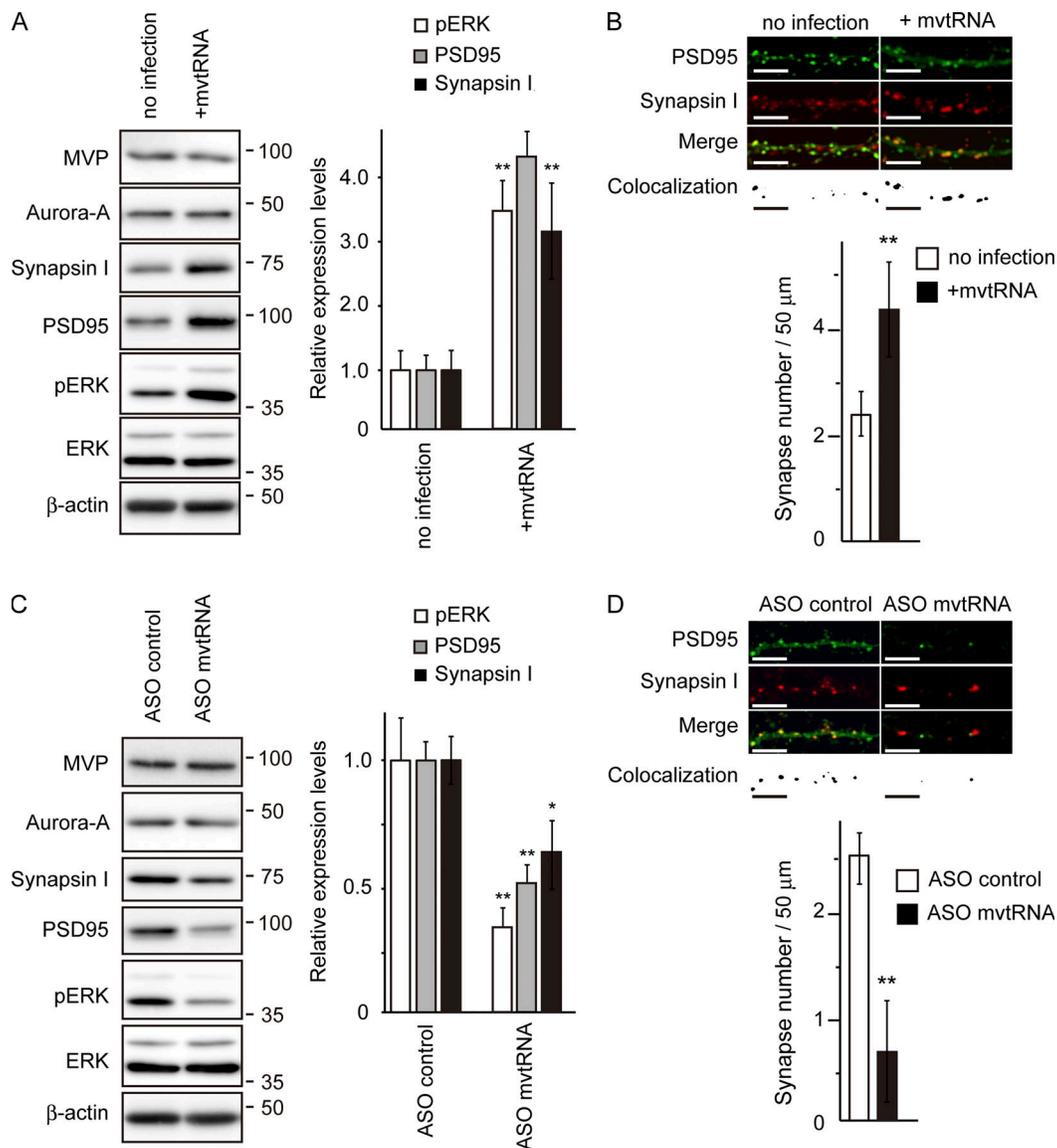
Figure 6. **The small noncoding mvtRNA enhances synapse formation by the activation of ERK signaling. (A and B)** Overexpression of mvtRNA enhances synapse formation by activation of ERK signaling. **(A)** Lysates were prepared from cultured cortical neurons infected with lentivirus overexpressing mvtRNA. Representative immunoblots for the expression of the indicated molecules are shown. β-Actin serves as a loading control. Phosphorylation levels of ERK (calculated as phosphorylated ERK/total ERK) and expression levels of Synapsin I or PSD95 normalized to β-actin relative to the control (no infection; mean ± SEM, n = 5) are shown. **(B)** Synapse formation was assessed by double immunostaining with antibodies against PSD95 and Synapsin I. Representative photomicrographs of cultured cortical neurons infected with lentivirus expressing mvtRNA at 14–16 DIV and the number of synapses per dendrite length wae shown. The colocalization panels show the double-positive puncta extracted from merged images that were identified as synapses (shown in black). Scale bar, 25 μm. **(C and D)** Down-regulation of mvtRNA suppresses synapse formation by interfering with the activation of ERK signaling. **(C)** Lysates were prepared from cultured cortical neurons transfected with ASO against mvtRNA. Representative immunoblots for the expression of the indicated molecules are shown. β-Actin serves as a loading control. Phosphorylation levels of ERK (calculated as phosphorylated ERK/total ERK) and expression levels of Synapsin I or PSD95 normalized to β-actin relative to the control (ASO control; mean ± SEM, n = 5) are shown. **(D)** Synapse formation was assessed by double immunostaining using antibodies against PSD95 and Synapsin I. Representative photomicrographs of cultured cortical neurons infected with lentivirus expressing mvtRNA at 14–16 DIV and the number of synapses per dendrite length are shown. The colocalization panels show the double-positive puncta extracted from the merged images that were identified as synapses (shown in black). Scale bar, 25 μm. Note that neither overexpression nor down-regulating expression of mvtRNA affects the expression of Aurora-A and MVP in cortical neurons. Significant differences from the control (*, P < 0.05; **, P < 0.01) were determined by one-way ANOVA with Tukey's post hoc test (A and C) or two-tailed Student's t test (B and D).

(Fig. 7 F). We found that overexpression of either WT Aurora-A or T288D, but not K153R, increases mvtRNA expression in S100 fractions, suggesting that Aurora-A–dependent phosphorylation of MVP up-regulates the levels of mvtRNA expression in the soluble cytoplasmic fraction of neurites.

Reduced MVP diminishes local translation activity in neurites

Our results shown above suggest that mvtRNA might function as a riboregulator of synaptogenesis by modulating the ERK signaling pathway. To correlate MVP-mediated transport of mvtRNA with local translation in neurites, we examined
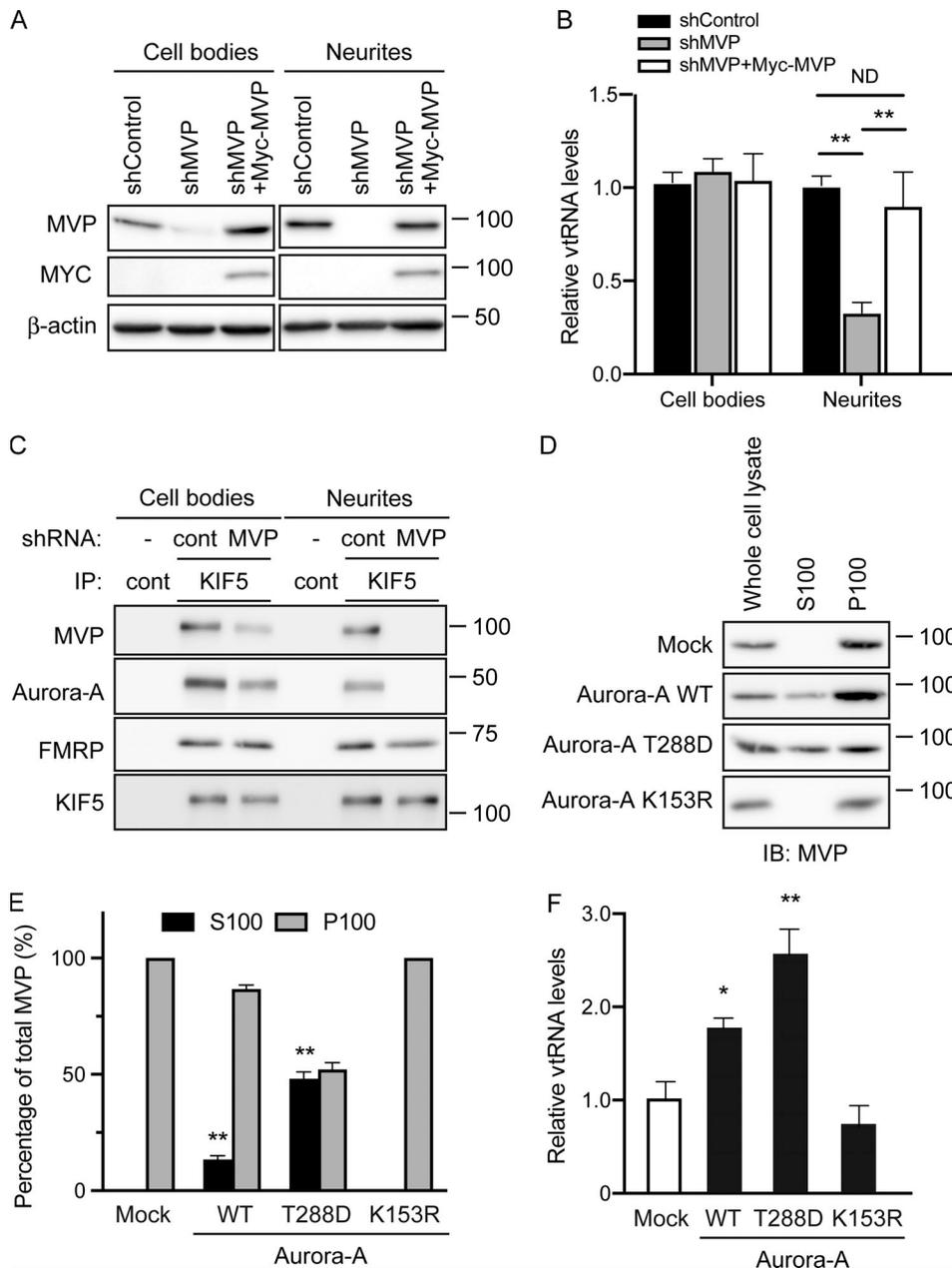
Figure 7. **mvtRNA is transported in neurites with the vault complex. (A and B)** The localization of mvtRNA in neurites is dramatically inhibited by the down-regulation of *mvp* expression. Lysates were prepared from cell bodies or neurites of cortical neurons infected with lentivirus expressing the indicated shRNA. Representative immunoblots for the expression of MVP are shown in A. β-actin serves as a loading control. Quantified expression levels of mvtRNA in S100 fractions from neurites by quantitative PCR relative to the level with shControl are shown in B. Note that the phenotypic change by RNAi was rescued by coexpression of shRNA-resistant MVP cDNA. **(C)** Interaction of KIF5 with the MVP–Aurora-A complex. The molecular interaction between KIF5 and the MVP–Aurora-A complex with the shRNA-mediated down-regulation of *mvp* expression was assessed by coimmunoprecipitation experiments using an anti-KIF5 antibody in lysates from neurites. Representative immunoblots and immunoprecipitation analyzed by immunoblotting with the indicated antibodies are shown. FMRP serves as positive control for interaction with KIF5. Note that down-regulation of *mvp* resulted in significantly decreased interaction between KIF5 and Aurora-A. **(D–F)** Aurora-A–dependent phosphorylation of MVP disrupts the integrity of the vault complex and thereby increases the levels of mvtRNA in neurites. Lysates were prepared from soma or neurites of cortical neurons infected with adenovirus vectors expressing HA-tagged Aurora-A WT, Aurora-A T288D, or Aurora-A K153R. Representative immunoblots for the expression of MVP are shown in D. β-Actin served as a loading control. Quantified expression levels of MVP between each fraction (S100 and P100) from neurites expressing HA-tagged Aurora-A WT, Aurora-A T288D, or Aurora-A K153R are shown in E. Quantified expression levels of mvtRNA in S100 fraction from neurites expressing HA-tagged Aurora-A WT, Aurora-A T288D, or Aurora-A K153R by quantitative PCR are shown in F. Significant differences from the control (*, $P < 0.05$; **, $P < 0.01$) were determined by one-way ANOVA with Tukey's post hoc test.

whether reduction of mvtRNA transport by RNAi-mediated *mvp* down-regulation affects local translation in neurites (Fig. 8). To this end, we included a transfer RNA analogue puromycin to metabolically label newly synthesized proteins, followed by immunoblot analysis to visualize puromycin-incorporated proteins representing newly synthesized proteins in neurites (Rangaraju et al., 2019). To quantify the local translation activity in neurites, mouse cortical neurons were cultured using a cell placement device (Fig. 8 A), and their neurites were assessed by immunoblot analysis. The puromycin-labeled proteins in the neurites of control neurons were found to appear in a smear manner. In contrast, lysates from neurites with RNAi-mediated reduction of *mvp* expression exhibited a significant decrease in puromycin-positive smears. mvtRNA down-regulation by transfecting ASOs also decreased the smears (Fig. 8, B and C). To visualize changes in puromycin incorporation in neurites, we performed immunocytochemistry to detect the incorporated puromycin in neurons. We found that puromycin immunoreactivity was significantly lower in neurites with the down-regulated expression of *mvp* than that in control neurites, and that the overexpression of shRNA-resistant cDNA of *mvp* rescued the effect of the down-regulated expression (Fig. 8, D and E). These results suggest that MVP reduction diminishes local translation activity in neurites. We also found that the neurites expressing ASOs against mvtRNA exhibited a reduction of puromycin immunoreactivity, further suggesting that mvtRNA may participate in the regulation of local translation in neurites.

mvtRNA directly interacts with MEK1 and thereby increases its kinase activity

Our current data suggest that vault complex–dependent mvtRNA transportation in neurites may serve as a downstream signaling event of Aurora-A activation and enhance the activation of ERK in the synaptic region. MEK is a regulatory component of the MAPK signaling pathway, and its target sites for phosphorylation are very limited, with most activity directed at ERK (Ordan et al., 2018; Seger et al., 1992; Yuan et al., 2018). Because previous studies have reported that vtRNA directly controls protein function, we hypothesized that mvtRNA can bind to and regulate MEK1. To explore the mvtRNA and MEK1 interaction in vitro, we examined whether biotinylated mvtRNA could be UV-cross-linked to a recombinant Myc-tagged MEK1. We found that MEK1 formed complexes with mvtRNA, but not human vtRNA2-1 (hvtRNA2-1; Fig. 9 A). To validate this observation, we performed RIP-qPCR (RNP immunoprecipitation followed by cDNA synthesis and quantitative real-time PCR) from cultured cortical neurons, using antibodies against MEK1 or ERK, respectively. We observed prominent and specific enrichment of mvtRNA in immunoprecipitates using an antibody against MEK1, but not ERK (Fig. 9, B and C). These results suggest that mvtRNA can interact with MEK1. As another way to show that mvtRNA interaction with MEK1 affects its kinase activity, we performed an in vitro kinase assay to demonstrate that mvtRNA-dependent MEK1 activation leads to an increase in ERK phosphorylation. Increase in ERK phosphorylation was significantly enhanced in the presence of mvtRNA (Fig. 9, D–F). These results suggest that mvtRNA directly interacts with MEK1 and thereby increases its kinase activity.

Discussion

We have shown here that the small noncoding vtRNA regulates synapse formation in murine cortical neurons to enhance its activity by direct interaction with MEK, a regulatory component of the MAPK signaling pathway (Fig. 10). MEK is a dual-specificity protein kinase that can phosphorylate both the threonine and tyrosine residues of ERK (Seger et al., 1992; Yuan et al., 2018). Much information has been accumulated about the relationship between the structure and activity of MEK. MEK has several domains with assigned functions and interaction partners but does not contain any typical RNA-binding motif. MEK also contains all of the functionally critical regions shared within protein kinases, including an activation loop, which interacts with residues outside the kinase domain and maintains the low basal activity of MEK by wrapping itself tightly around the catalytic pocket (Ordan et al., 2018). MEK activation is achieved once its two serine residues within the activation loop are phosphorylated by an activating kinase, such as Raf kinase (Morrison and Davis, 2003). Thus, MEK activity can be altered not only by modification to kinase domain residues, but also by structural changes in the activation loop. hvtRNA1-1 has been reported to directly regulate selective autophagy by binding to the autophagy receptor p62 (also known as sequestosome-1) and thereby interfering with its oligomerization (Horos et al., 2019). p62 binds to specific autophagic substrates via interaction with Atg8-like proteins, including LC3B, and transports them to the autophagosome membrane. Among the autophagic receptors, p62 has a unique property of oligomerization, which increases its affinity to autophagosome membranes and is thought to help align p62 with the formation of autophagosome structure. As in this example, mvtRNA appears to inhibit the interaction of the activation loop with the kinase domain and thereby enhances the kinase activity of MEK. We also found that suppression of mvtRNA expression by ASO did not completely suppress ERK activity or synaptogenesis, which may reflect a regulatory role of mvtRNA on MEK activity. These results suggest that mvtRNA might not function as an "on–off switch" of MEK activity, but rather as a regulator. If the mechanism by which MEK1 is activated by mvtRNA can be clarified in the future, novel findings may be uncovered by comparison with the activation mechanism of MEK1 by phosphorylation.

Our results suggest that the kinase activity of Aurora-A strongly affects the distribution of mvtRNA in neurites and up-regulates the levels of mvtRNA expression in the soluble cytoplasmic fraction of neurites (Fig. 10). The cytoplasmic polyadenylation element (CPE)-containing mRNAs in dendrites, including α-Ca²⁺/calmodulin-dependent protein kinase II, are known to be polyadenylated in a neural activity-dependent manner and translated at synaptic sites (Huang et al., 2003; Martin, 2004). Huang et al. (2002) reported that neural activity–dependent translational regulation in the synaptic region is controlled by phosphorylation of the CPE binding (CPEB) protein by Aurora-A. Indeed, N-Methyl-D-aspartate-dependent
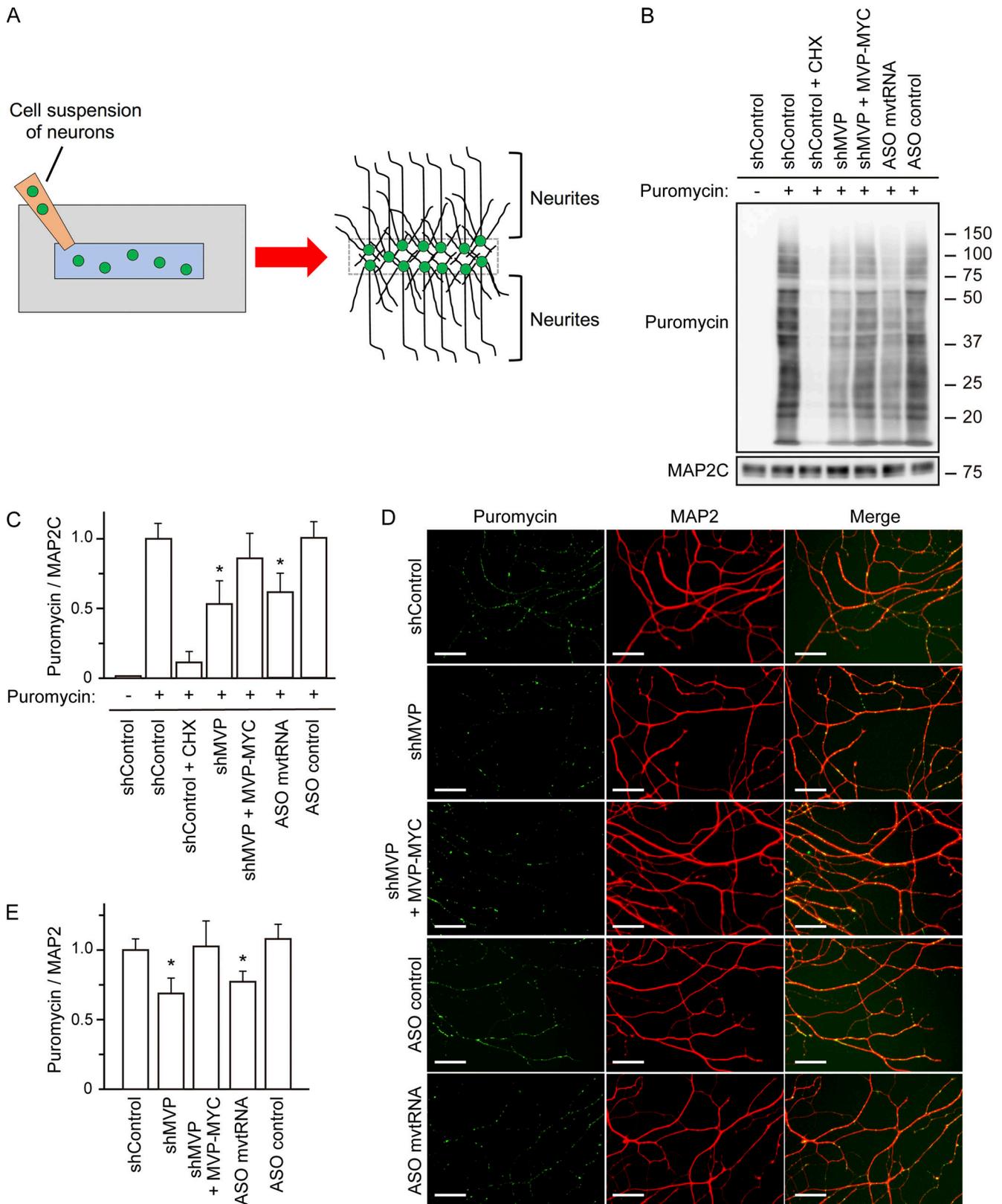
Figure 8. **Reduction of MVP expression decreases local translational activity in neuritis. (A)** Schematic diagram of compartmentalized cultures of neuronal cell bodies and neurites (axons and dendrites). The gray rectangle with a blue slit in the center indicates a cell placement device, and the orange triangle indicates the neuron-containing media. The green circles indicate a neuron. **(B and C)** Expression analysis of puromycin-incorporated proteins in neurites of cortical neurons. Representative images of immunoblots (B) and quantified intensities of puromycin immunoreactivity relative to MAP2C immunoreactivity normalized to the level of shControl (C; mean ± SEM, n = 3 in each group from three independent experiments). *, P < 0.05 compared with neurons

expressing nontarget control shRNA by one-way ANOVA test and Tukey's multiple comparisons test. Note that the band density of proteins becomes weakened with shRNA-mediated down-regulation of *mvp* expression. Puromycin-incorporated proteins were not detected in cycloheximide-treated neurites. **(D and E)** Representative photomicrographs of puromycin-incorporated proteins in neurites of cultured cortical neurons (stained in green; counterstained with MAP2 in red) are shown in D, and quantified levels of puromycin immunoreactivity against MAP2 immunoreactivity normalized to the level of shControl are shown in E (mean ± SEM, n = 12 in each group from three independent experiments). Scale bar, 50 μm. Significant differences from the level of shControl (*, P < 0.05) were determined by one-way ANOVA with Tukey's post hoc test.

neural activation is known to increase phosphorylation of CPEB protein by Aurora-A kinase, suggesting that Aurora-A kinase activity might be regulated by synaptic activity. These findings suggest that Aurora-A involvement in the regulation of synaptogenesis is likely caused by intracellular signaling elicited by synaptic activity.

Previous reports have suggested that MVPs may be transported in neurites by fast transporters (Herrmann et al., 1999; Li et al., 1999). MVPs have also been reported to associate with several mRNAs that are translated within dendrites, including tissue plasminogen activator and striatal-enriched tyrosine phosphatase (Paspalas et al., 2009). In the current study, we revealed that the MVP–Aurora-A complex was transported in the neurites by the kinesin superfamily protein KIF5. KIF5 is involved in axonal transport of various cargos and also participates in the proper targeting of mRNA and associated proteins in dendrites (Hirokawa, 2006). These and our results suggest that the MVP–Aurora-A complex may function as a cargo transporter of mRNAs translated in the dendrites and of its interacting molecules involved in the local translation, including Aurora-A and vtRNA.

Some studies have suggested a link between vtRNAs and the regulation of synaptic function. NOP2/Sun domain family member 2 is a methyltransferase that introduces 5-methylcytosine into small ncRNAs including vtRNA (Hussain and Bashir, 2015; Hussain et al., 2013). The absence of NOP2/Sun domain family member 2–mediated methylation reduces the expression level of calcium voltage-gated channel auxiliary subunit γ 8 gene, which regulates AMPA receptor transport and channel gating. Dysregulation of vtRNAs has been linked with neurological disorders such as intellectual disability, although the contribution of vtRNAs in this process remains unclear. MAPK signaling is required for spine formation, for various forms of synaptic plasticity, and for learning and memory (Sweatt, 2004; Thomas and Huganir, 2004). Our findings that mvtRNA modulates synapse formation by amplifying MAPK signaling may facilitate the identification of novel therapeutic targets for the treatment of synaptic dysfunction (Fig. 10).

Recent studies have identified RNA-binding capability in many proteins that have not previously been detected as RNA-binding proteins (Hentze et al., 2018). Many such proteins lack typical RNA-binding motifs, and therefore their physiological function remains unclear. We have shown that the protein kinase MEK is an RNA-binding protein whose kinase activity is regulated by mvtRNA even though MEK has no typical RNA-binding motif. The regulation of MEK activity by mvtRNA is initiated by Aurora-A–dependent MVP phosphorylation. The regulation of various protein functions by small ncRNAs has

previously been reported by others. In bacteria, the ~180–200-nt-long 6S RNA binds to RNA polymerase and regulates its function during stationary growth (Wassarman and Storz, 2000). In mammalian cells, hvtRNA1-1 acts as a regulator of selective autophagy by binding directly to the autophagy receptor p62 (Horos et al., 2019). Further identification of essential roles of vtRNA in the regulation of protein function, and also the mechanisms regulating its expression, will provide unique insights into its role in development and also potential roles in pathogenesis of diseases.

Materials and methods

Animals
All animals were maintained in accordance with the guidelines of the National Center for Neurology and Psychiatry. The technical protocols for animal experiments in this study were approved by a review committee for animal resources in the National Center for Neurology and Psychiatry.

Antibodies
The antibodies used and their sources are as follows: mouse anti–β-actin antibody (622101; BioLegend); mouse anti–HA-tag antibody (MMS-101R; Covance); mouse anti–MYC-tag antibody (clone 9E10; DSHB); mouse anti-FMRP antibody (clone 7G1-1; DSHB); mouse anti–His-tag antibody (clone OGHis; MBL); mouse anti–Aurora-A antibody (clone 35C1; Abcam); rabbit anti-ERK antibody (4695; Cell Signaling); rabbit anti–phospho-ERK antibody (4377; Cell Signaling); rabbit anti-AKT antibody (9272; Cell Signaling); rabbit anti–phospho-AKT antibody (9271; Cell Signaling) ; mouse anti-PSD95 antibody (MA1-046; Thermo Fisher Scientific); guinea pig anti-PSD95 antiserum (124 014; Synaptic Systems); mouse anti–Synapsin I antibody (MAB355; Millipore); guinea pig anti-VGLUT1 antibody (AB5905; Millipore); rabbit anti-MAP2 antibody (M3696; Merck); mouse anti-phosphoserine antibody (clone 4A4; Millipore); rabbit anti-phosphothreonine antibody (clone 42H4; Cell Signaling); rabbit anti-phosphoserine antibody (2630; Cell Signaling); rabbit anti-KIF3 antibody (ab11259; Abcam); rabbit anti-KIF5 antibody (ab62104; Abcam); and mouse anti-puromycin antibody (clone 12D10; Millipore). HRP-conjugated (Vector Laboratories), Alexa Fluor 565–conjugated, and Alexa Fluor 488–conjugated (Molecular Probes) antibodies were used as secondary antibodies for detection.

For generation of the antiserum for MVP, a synthetic peptide corresponding to amino acids 754–766 (KLKAQALAIETEA) of mouse MVP was used to immunize rabbits following standard procedures (Thermo Fisher Scientific). Immunoglobulin reactive for the antigen peptide was purified by an affinity column using the antigen peptide. The specificity of the affinity-purified
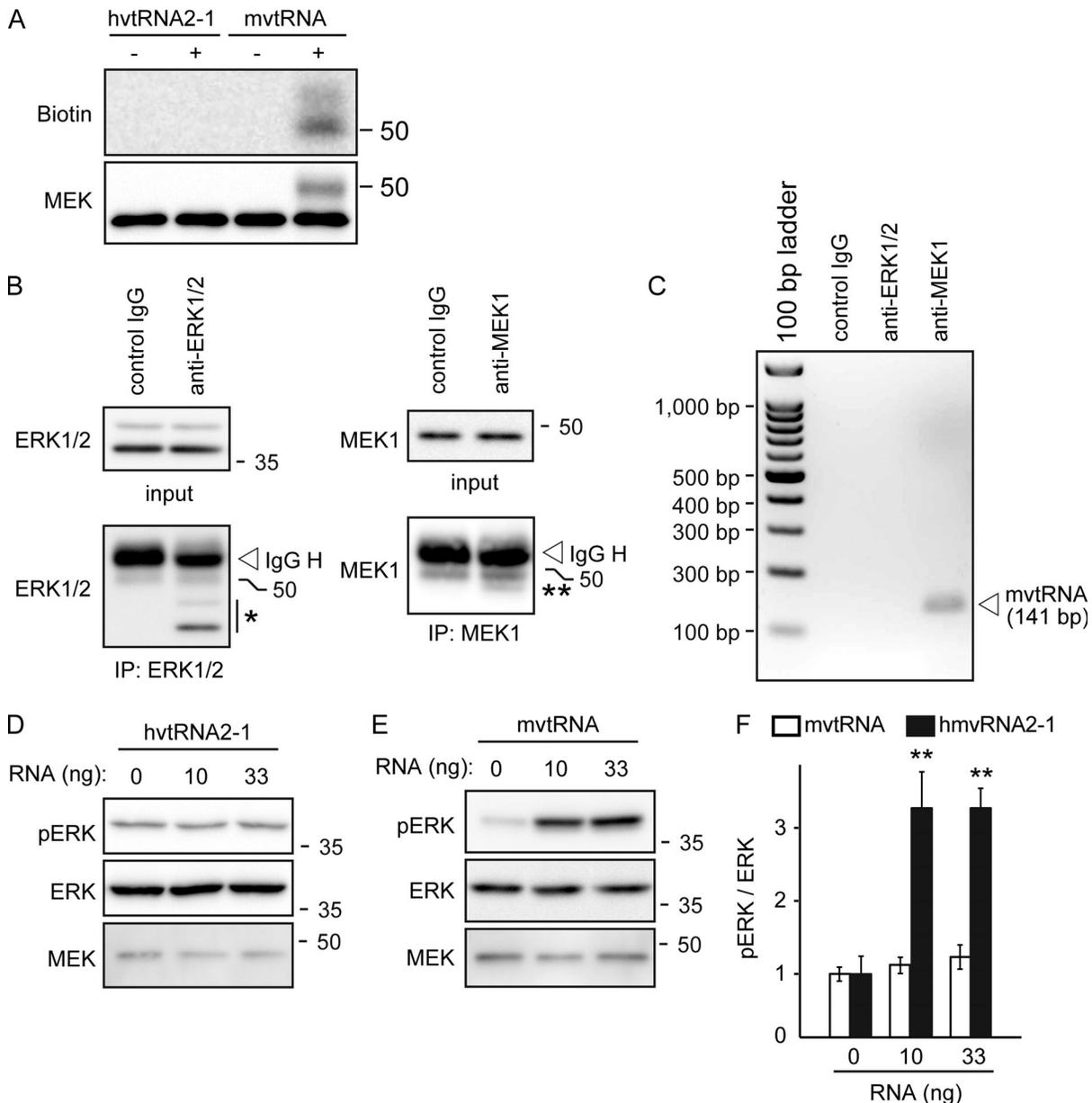
Figure 9. **mvtRNA directly interacts with MEK1 and thereby increases its kinase activity. (A)** mvtRNA interacts with MEK1 in vitro. Biotinylated mvtRNA was UV-cross-linked to and coimmunopurified with a recombinant Myc-tagged MEK1. Representative blots for biotin and MEK1 for each condition are shown. **(B and C)** RIP-qPCR from cultured cortical neurons. Representative immunoprecipitations using antibodies against MEK1 or ERK are shown in B. Existence of mvtRNA in the immunoprecipitates using the indicated antibodies was assessed by agarose gel electrophoresis in C. Note that prominent and specific enrichment of mvtRNA is observed in immunoprecipitates using an antibody against MEK1, but not ERK. **(D–F)** mvtRNA up-regulates MEK activity in vitro. In vitro kinase assays were performed using recombinant MEK1 and ERK together with mvtRNA or hvtRNA2-1. Assay mixtures were incubated for 3 h at 30°C and subjected to immunoblot analysis using the indicated antibodies. Phosphorylation levels of ERK (calculated as phosphorylated ERK/total ERK) relative to the control (no mvtRNA addition, 0; mean ± SEM, n = 5) are shown in F. Significant differences from the control (**, $P < 0.01$) were determined by one-way ANOVA with Tukey's post hoc test. IP, immunoprecipitation.

anti-MVP antibody was confirmed by immunoblot analysis with lysates of Neuro-2a cells expressing MVP.

Preparation of synaptosome and PSD fractions

PSD and synaptosome fractions were isolated from mouse brains as previously described (Araki and Milbrandt, 2003). All buffers contained a protease inhibitor cocktail (Nacalai Tesque), and all procedures were performed on ice or at 4°C. Briefly, mouse brains were homogenized in 0.32 M sucrose and 4 mM Hepes (pH 7.4) and centrifuged at 1,000 g to remove the pelleted nuclear fraction and debris. The supernatant was collected and centrifuged at 10,000 g for 15 min. The resulting supernatant and pellet were collected as cytosol and crude membrane fractions, respectively. The membrane fraction pellet was lysed by hypoosmotic shock in 4 mM Hepes (pH 7.4) and centrifuged at 25,000 g for 20 min. The resulting pellet was resuspended in
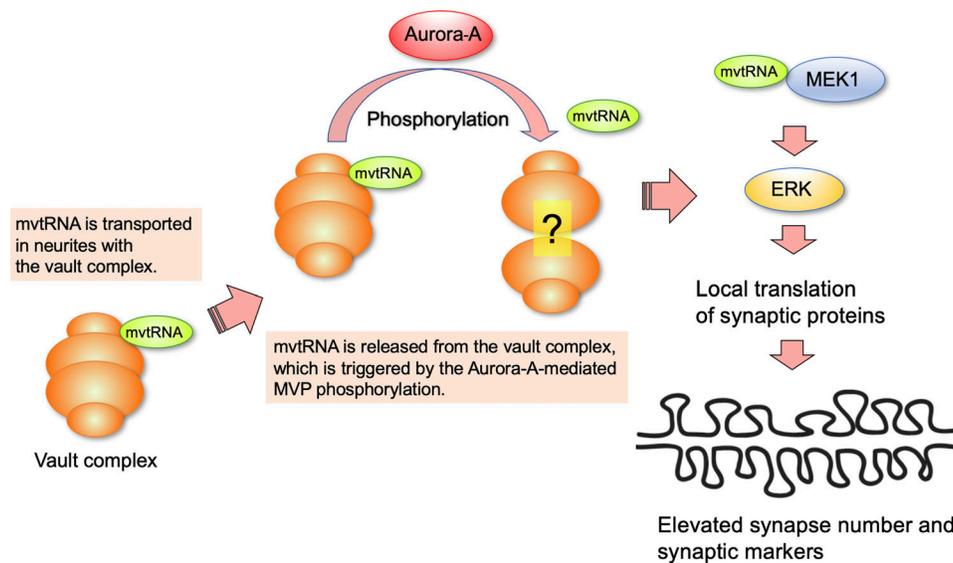
Figure 10. **The vault RNA modulates synapse formation by amplifying MAPK signaling.** mvtRNA is transported to the distal regions of the neurites as part of the vault complex. mvtRNA is released from the vault complex in the neurite by a mitotic kinase Aurora-A–dependent phosphorylation of MVP, a major protein component of the vault complex. mvtRNA binds to and activates MEK1, thereby enhancing MEK1-mediated ERK activation in neurites. Activation of ERK signaling promotes local translation of synaptic proteins, which accelerates synapse formation. Thus, vtRNA functions as a putative riboregulator of synaptogenesis.

50 mM Hepes (pH 7.4) and 2 mM EDTA and regarded as the synaptosome fraction. To obtain PSD fractions, Triton X-100 (final concentration 0.5%) was added to the supernatant, rotated for 15 min, and centrifuged at 32,000 g for 20 min. The resultant pellet was resuspended in 50 mM ice-cold Hepes (pH 7.4) and 2 mM EDTA, mixed with Triton X-100 (final concentration 0.5%) for 15 min, and centrifuged at 200,000 g for 20 min. The resultant pellet was resuspended in 50 mM Hepes (pH 7.4) and 2 mM EDTA and regarded as the PSD fraction.

Cortical neuron culture
Cerebral hemispheres were removed separately from embryonic day 14–16 C56BL/6J mice. Cells were dissociated with papain and seeded at a density of 4×10^5 cells/well onto 24-well plates coated with poly-L-lysine (Merck) and laminin (Merck) in DMEM containing 10% FBS. From the third day in vitro (DIV), the cells were maintained in Neuro-medium (Miltenyi Biotec) containing 2% Neuro-Brew-21 (Miltenyi Biotec) and 1 mM GlutaMAX (Thermo Fisher Scientific). The cells were cultured for 14–16 d and used for immunoblot or immunostaining experiments.

Neurite preparation
Neurite preparation was performed as previously described (Wakatsuki et al., 2015). Briefly, cell culture inserts were coated with poly-L-lysine and laminin at 4°C overnight and were placed in a well containing 2 ml culture medium in a six-well plate. The inside of the insert was filled with 1 ml medium. Cortical neurons (5×10^5 cells) were placed within the inserts and cultured as described above. Neurite samples were obtained from the bottom surface of the insert and used for biochemical analyses. For analysis of local translation in neurites, a cell placement device

with a 5 × 1-mm rectangular seeding area in the center was made using a polydimethylsiloxane prepolymer kit (Sylgard 184 silicon elastomer; Dow Corning). Dissociated mouse cortical neurons were seeded into the rectangular area. After 7–10 DIV, the cell bodies were all positioned within the rectangular area, while their neurites extended perpendicular to the long axis of the rectangular cell body area. After the medium was removed from the culture wells, conditioned medium containing 10 µg/ml puromycin and/or 100 µM cycloheximide was added and cultured for 2 h. After incubation and washing once with PBS, the neurites were collected using an 18-gauge needle to be lysed for immunoblotting or fixed with 4% PFA for morphological analysis.

Immunoblot and immunoprecipitation
For immunoblot analysis, cultured cells or tissues were homogenized in radioimmunoprecipitation assay buffer (1% Triton X-100, 0.5% sodium deoxycholate, 0.1% SDS, 150 mM NaCl, and 50 mM Tris–HCl, pH 7.5) containing phosphatase (07574-61; Nacalai Tesque) and protease (25955-11; Nacalai Tesque) inhibitor cocktails. Equal amounts of protein were separated by SDS-PAGE, followed by immunoblotting. Immunoreactivity was visualized by using HRP-conjugated secondary antibodies and a chemiluminescent substrate (Wako Chemical). The chemiluminescent images were captured by LAS4000-mini and quantified using ImageJ software. Scans at multiple exposures were obtained to ensure that the results fell within the linear range of the instrument.

For immunoprecipitation, cells or tissues were lysed in a lysis buffer (1% Triton X-100, 100 mM NaCl, and 20 mM Tris–HCl, pH 7.5) containing protease inhibitor cocktail. After centrifugation at 15,000 g for 30 min, the supernatant was incubated at 4°C overnight with the primary antibody. After incubation with

protein A–coupled Dynabeads, proteins were eluted by boiling for 5 min in Laemmli sample buffer and analyzed by immunoblotting.

For identification of MVP, the immunoprecipitates were separated by SDS-PAGE, and the gels were subsequently analyzed by silver staining (Atto). The band corresponding to 100 kD was excised from a silver-stained gel. The identity of the band was determined by peptide mass fingerprinting analysis on a MALDI-TOF mass spectrometer.

Plasmid construction and mutagenesis
The coding region of MVP or Aurora-A was amplified by PCR using LA-taq (Takara Bio) from corresponding cDNA clones (GenBank accession numbers NM_080638 for murine MVP and NM_011497 for murine Aurora-A) and cloned into indicated expression constructs. The integrity of each clone was confirmed by sequencing. Regarding detection, a His tag or MYC tag was added to the C terminus of MVP, and an HA tag was added to the C-terminus of Aurora-A. Aurora-A mutants (T288D and K153R) were generated by PCR-mediated site-directed mutagenesis, and an HA tag was added at the C terminus. mvtRNA and hvtRNA2-1 were amplified by PCR using LA-taq from mouse brain cDNA library and cloned into pLKO.1.

Viral vectors and infection
Viral vectors were generated using AxCALNLwtit2 cosmid vector (Takara Bio) essentially as previously described (Wakatsuki et al., 2011; Wakatsuki et al., 2017). cDNAs for Aurora-A HA, Aurora-A HA T288D, Aurora-A HA K153R, and MYC-MVP were constructed as described above. A recombinant adenovirus was generated using the Takara adenovirus expression kit (Takara Bio) following the manufacturer's instructions. The purification and concentration of adenoviral vectors was achieved and measured by two rounds of cesium chloride density gradient centrifugation and Centricon Centrifugal Filter Devices (Millipore), respectively, according to the manufacturers' instructions. Viral titers were measured by a plaque-forming assay in HEK293 cells.

For experiments using lentiviral vectors, control and specific shRNAs in the pLKO.1 puromycin-resistant lentiviral vector were purchased from Merck. We used the BLOCK-iT RNAi designer (Thermo Fisher Scientific) to select target sequences. We designed target sequences directed against the UTR. The following shRNA oligonucleotides were used: MVP, 5′-CACCGG AAGTCATCCCAAGTGTTGGCGAACCAACACTTGGGATGACTT CC-3′; and Aurora-A, 5′-CACCGGAGAACCTTTGAATTGTAACCG AAGTTACAATTCAAAGGTTCTCC-3′.

We used SHC002 for the nontarget control shRNA. Constructs for mvtRNA and hvtRNA2-1 were generated as described above. Lentiviral packaging was performed using HEK293FT cells as previously described (Wakatsuki et al., 2011).

ASOs
The ASOs used in this study were designed as published previously (Nandy et al., 2009). The ASOs were mixed oligonucleotides having 5 or 6 nt on each end substituted with 2′-O-methyl ribonucleotides. The sequences of ASOs targeting mvtRNA and

nontarget controls were as follows: ASO nontarget control, 5′-TCACCTTCACCCTCTCCACT-3′; ASO-mvtRNA1, 5′-GGGTTA GGTAAGTGGTTGGTTGTGT-3′; ASO-mvtRNA2, 5′-GCTGGCCCG TCTATCTCTTCCTGGA-3′; and ASO-mvtRNA3, 5′-CGGGTTAGG TAAGTGGTTGG-3′.

For ASO transfection, cells were seeded at a density of 10⁶ cells/ well onto six-well plates and cultured as described above. Control or targeting ASOs for mvtRNA were transfected into cultured neurons using DharmaFECT1 transfection reagent according to the manufacturer's protocol (Thermo Fisher Scientific).

Analysis of interaction between mvtRNA and MEK1
For MEK1 RIP-qPCR, the immunoprecipitates obtained by using anti-MEK1 antibody were directly resuspended in TRI reagent (T9424; Merck). RNA in the immunoprecipitates was purified according to the manufacturer's protocol and used for cDNA synthesis as described above. mvtRNA and hvtRNA2-1 were synthesized with a 5′ biotinylation modification (Genedesign). Recombinant MEK1 protein was incubated with mvtRNA in reaction buffer (10 mM Hepes, 3 mM MgCl$_2$, 14 mM KCl, 5% glycerol, 0.2% NP-40, and 1 mM DTT) for 30 min at room temperature. The mixture was transferred onto parafilm, placed on ice 1–2 cm from the UV light source (254 nm), and cross-linked using a Gene Linker UV-cross-linking apparatus (Bio-Rad) for 30 min. Finally, samples were mixed 1:1 with 2× SDS-PAGE sample buffer and heated at 100°C for 5 min. The reactions were separated by SDS-PAGE followed by blotting to PVDF membrane. Reactivity was visualized by using HRP-conjugated streptavidin and chemiluminescent substrate.

qPCR
Total RNA was extracted from cultured cortical neurons or Neuro-2a cells using the RNeasy MiniKit (Qiagen). qPCR was performed as previously described using the Applied Biosystems Prism model 7300 sequence detection instrument and a standard SYBR green detection protocol. The sequences of the PCR primers using the SYBR green method are as follows: β-actin forward, 5′-CCCCCAATGTATCCGTTGTG-3′; β-actin reverse, 5′-CCAGTTGGTAACAATGCCATGT-3′; MVP forward, 5′-ATC CGGCAGGACAATGAGAG-3′; MVP reverse, 5′-TATCTTCAAAGT CCAGCAATGC-3′; Aurora-A forward, 5′-CTGGATGCTGCAAAC GGATAG-3′; Aurora-A reverse, 5′- CGAAGGGAACAGTGGTCT TAACA-3′; mvtRNA forward, 5′-CAGCTTTAGCTCAGCGGTTAC-3′; mvtRNA reverse, 5′-AAGGGCCAGGGAGCGCCCGC-3′.

The samples were run in duplicate. The expression level for each gene of interest was normalized to that of β-actin.

Imaging of intracellular Ca²⁺
Primary cortical cultures were prepared from postnatal 2-d-old rats as previously reported (Numakawa et al., 2009). Ca²⁺ imaging using fluo-3 dye was performed as previously reported (Numakawa et al., 2009; Yagasaki et al., 2006). Neurons were cultured on polyethylenimine-coated cover glass (Matsunami) attached to flexiperm. A fluorescent microscope (Axiovert 200 controlled by Slide Book 3.0; Zeiss) was used to monitor the fluo-3 dye intensity. The data were analyzed using Slide Book 3.0 (Intelligent Imaging Innovations). Quantitative data were obtained from the analysis of each randomly selected cell body

Wakatsuki et al.
Vault RNA modulates synapse formation

Journal of Cell Biology 16 of 19
https://doi.org/10.1083/jcb.201911078

because we detected a higher intensity of fluo-3 dye emission in the cell bodies than in the neurites. All imaging experiments were performed at least three times on separate cultures. Representative images from neurons in a sister culture are shown in the figures.

FM4-64FX labeling

Mouse cortical neurons on coverslips were infected with adenovirus for expression of indicated molecules at 14–16 DIV. After 2 d, cells were loaded with 10 µM FM4-64FX dye (F34653; Thermo Fisher Scientific) in depolarizing buffer (100 mM NaCl, 50 mM KCl, 2 mM CaCl$_2$, 1 mM MgCl$_2$, 10 mM glucose, and 15 mM Hepes, pH 7.3) for 1 min to load vesicles. Coverslips were then transferred to wash buffer (140 mM NaCl, 5 mM KCl, 2 mM CaCl$_2$, 1 mM MgCl$_2$, 10 mM glucose, and 15 mM Hepes, pH 7.3) for 5 min to remove excess dye and fixed in 4% PFA for 10 min. After fixation, coverslips were washed with PBS and mounted with Vectashield. To quantify FM4-64FX uptake per synaptic puncta, we analyzed three separate coverslips of cultured neurons and acquired 10 images per condition in each experiment. The intensity of FM4-64FX dye labeling at each Synapsin I–positive punctum was measured using ImageJ software.

Microscopy image acquisition

In the immunocytochemical analysis of cultured cortical neurons, cells were fixed with 4% PFA in PBS and then permeabilized with 0.2% Triton X-100 in PBS. Incubation with primary antibody was performed at 4°C overnight, followed by secondary antibody at room temperature for 1 h. Specimens were mounted using Vectashield mounting medium (Vector Laboratories). Immunofluorescence was observed under an inverted microscope (DMI 6000B; Leica) and analyzed using LAS AF software (v3.2; Leica). Images were taken with a constant exposure time between all the conditions of the same experiment and processed using Photoshop software (Adobe).

For synaptogenesis experiments, 14-d cultures were immunostained using antibodies against MAP2 and PSD95. The MAP2 images were used to define the dendrites. The number of PSD95-labeled puncta per 50-µm length of dendrites expressing the indicated molecules ($n = 5$ for each condition) was counted for quantification in each sample.

Statistical analysis

Results are expressed as mean ± SEM. All statistical analyses in this study were performed using two-tailed Student's t test for single comparisons or one-way ANOVA analysis for multiple comparison in GraphPad Prism 8. Data distribution was assumed to be normal but was not formally tested.

Online supplemental material

Fig. S1 demonstrates that Aurora-A interacts with MVP in Neuro2-a cells. Fig. S2 shows that Aurora-A in concert with MVP enhances ERK signaling in Neuro2-a cells. Fig. S3 shows the down-regulation of the indicated genes by the specific shRNA or ASO in cultured cortical neurons. Fig. S4 demonstrates that the interaction of KIF3 with the MVP–AuroraA complex was not detected in cultured cortical neurons.

References

Amaral, P.P., M.E. Dinger, T.R. Mercer, and J.S. Mattick. 2008. The eukaryotic genome as an RNA machine. *Science.* 319:1787–1789. https://doi.org/10.1126/science.1155472

Araki, T., and J. Milbrandt. 2003. ZNRF proteins constitute a family of presynaptic E3 ubiquitin ligases. *J. Neurosci.* 23:9385–9394. https://doi.org/10.1523/JNEUROSCI.23-28-09385.2003

Barnes, A.P., and F. Polleux. 2009. Establishment of axon-dendrite polarity in developing neurons. *Annu. Rev. Neurosci.* 32:347–381. https://doi.org/10.1146/annurev.neuro.31.060407.125536

Barry, G., J.A. Briggs, D.P. Vanichkina, E.M. Poth, N.J. Beveridge, V.S. Ratnu, S.P. Nayler, K. Nones, J. Hu, T.W. Bredy, et al. 2014. The long noncoding RNA Gomafu is acutely regulated in response to neuronal activation and involved in schizophrenia-associated alternative splicing. *Mol. Psychiatry.* 19:486–494. https://doi.org/10.1038/mp.2013.45

Berger, W., E. Steiner, M. Grusch, L. Elbling, and M. Micksche. 2009. Vaults and the major vault protein: novel roles in signal pathway regulation and immunity. *Cell. Mol. Life Sci.* 66:43–61. https://doi.org/10.1007/s00018-008-8364-z

Blaker-Lee, A., S. Gupta, J.M. McCammon, G. De Rienzo, and H. Sive. 2012. Zebrafish homologs of genes within 16p11.2, a genomic region associated with brain disorders, are active during brain development, and include two deletion dosage sensor genes. *Dis. Model. Mech.* 5:834–851. https://doi.org/10.1242/dmm.009944

Bodrikov, V., A. Pauschert, G. Kochlamazashvili, and C.A.O. Stuermer. 2017. Reggie-1 and reggie-2 (flotillins) participate in Rab11a-dependent cargo trafficking, spine synapse formation and LTP-related AMPA receptor (GluA1) surface exposure in mouse hippocampal neurons. *Exp. Neurol.* 289:31–45. https://doi.org/10.1016/j.expneurol.2016.12.007

Carmena, M., and W.C. Earnshaw. 2003. The cellular geography of aurora kinases. *Nat. Rev. Mol. Cell Biol.* 4:842–854. https://doi.org/10.1038/nrm1245

Cochilla, A.J., J.K. Angleson, and W.J. Betz. 1999. Monitoring secretory membrane with FM1-43 fluorescence. *Annu. Rev. Neurosci.* 22:1–10. https://doi.org/10.1146/annurev.neuro.22.1.1

Gebetsberger, J., and N. Polacek. 2013. Slicing tRNAs to boost functional ncRNA diversity. *RNA Biol.* 10:1798–1806. https://doi.org/10.4161/rna.27177

Gilbert, J., and H.Y. Man. 2017. Fundamental Elements in Autism: From Neurogenesis and Neurite Growth to Synaptic Plasticity. *Front. Cell. Neurosci.* 11:359. https://doi.org/10.3389/fncel.2017.00359

Hentze, M.W., A. Castello, T. Schwarzl, and T. Preiss. 2018. A brave new world of RNA-binding proteins. *Nat. Rev. Mol. Cell Biol.* 19:327–341. https://doi.org/10.1038/nrm.2017.130

Herrmann, C., E. Golkaramnay, E. Inman, L. Rome, and W. Volknandt. 1999. Recombinant major vault protein is targeted to neuritic tips of PC12 cells. *J. Cell Biol.* 144:1163–1172. https://doi.org/10.1083/jcb.144.6.1163

Hirokawa, N. 2006. mRNA transport in dendrites: RNA granules, motors, and tracks. *J. Neurosci.* 26:7139–7142. https://doi.org/10.1523/JNEUROSCI.1821-06.2006

Horos, R., M. Büscher, R. Kleinendorst, A.M. Alleaume, A.K. Tarafder, T. Schwarzl, D. Dziuba, C. Tischer, E.M. Zielonka, A. Adak, et al. 2019. The Small Non-coding Vault RNA1-1 Acts as a Riboregulator of Autophagy. *Cell.* 176:1054–1067.e12. https://doi.org/10.1016/j.cell.2019.01.030

Huang, Y.S., J.H. Carson, E. Barbarese, and J.D. Richter. 2003. Facilitation of dendritic mRNA transport by CPEB. *Genes Dev.* 17:638–653. https://doi.org/10.1101/gad.1053003

Huang, Y.S., M.Y. Jung, M. Sarkissian, and J.D. Richter. 2002. N-methyl-D-aspartate receptor signaling results in Aurora kinase-catalyzed CPEB phosphorylation and alpha CaMKII mRNA polyadenylation at synapses. *EMBO J.* 21:2139–2148. https://doi.org/10.1093/emboj/21.9.2139

Hussain, S., and Z.I. Bashir. 2015. The epitranscriptome in modulating spatiotemporal RNA translation in neuronal post-synaptic function. *Front. Cell. Neurosci.* 9:420. https://doi.org/10.3389/fncel.2015.00420

Hussain, S., A.A. Sajini, S. Blanco, S. Dietmann, P. Lombard, Y. Sugimoto, M. Paramor, J.G. Gleeson, D.T. Odom, J. Ule, and M. Frye. 2013. NSun2-mediated cytosine-5 methylation of vault noncoding RNA determines its processing into regulatory small RNAs. *Cell Rep.* 4:255–261. https://doi.org/10.1016/j.celrep.2013.06.029

Hüttenhofer, A., P. Schattner, and N. Polacek. 2005. Non-coding RNAs: hope or hype? *Trends Genet.* 21:289–297. https://doi.org/10.1016/j.tig.2005.03.007

Kedersha, N.L., and L.H. Rome. 1986. Isolation and characterization of a novel ribonucleoprotein particle: large structures contain a single species of small RNA. *J. Cell Biol.* 103:699–709. https://doi.org/10.1083/jcb.103.3.699

Khazaei, M.R., and A.W. Püschel. 2009. Phosphorylation of the par polarity complex protein Par3 at serine 962 is mediated by aurora a and regulates its function in neuronal polarity. *J. Biol. Chem.* 284:33571–33579. https://doi.org/10.1074/jbc.M109.055897

Kickhoefer, V.A., K.S. Rajavel, G.L. Scheffer, W.S. Dalton, R.J. Scheper, and L.H. Rome. 1998. Vaults are up-regulated in multidrug-resistant cancer cell lines. *J. Biol. Chem.* 273:8971–8974. https://doi.org/10.1074/jbc.273.15.8971

Kickhoefer, V.A., S.K. Vasu, and L.H. Rome. 1996. Vaults are the answer, what is the question? *Trends Cell Biol.* 6:174–178. https://doi.org/10.1016/0962-8924(96)10014-3

Kim, E., S. Lee, M.F. Mian, S.U. Yun, M. Song, K.S. Yi, S.H. Ryu, and P.G. Suh. 2006. Crosstalk between Src and major vault protein in epidermal growth factor-dependent cell signalling. *FEBS J.* 273:793–804. https://doi.org/10.1111/j.1742-4658.2006.05112.x

Kolli, S., C.I. Zito, M.H. Mossink, E.A. Wiemer, and A.M. Bennett. 2004. The major vault protein is a novel substrate for the tyrosine phosphatase SHP-2 and scaffold protein in epidermal growth factor signaling. *J. Biol. Chem.* 279:29374–29385. https://doi.org/10.1074/jbc.M313955200

Lee, K., N. Kunkeaw, S.H. Jeon, I. Lee, B.H. Johnson, G.Y. Kang, J.Y. Bang, H.S. Park, C. Leelayuwat, and Y.S. Lee. 2011. Precursor miR-886, a novel noncoding RNA repressed in cancer, associates with PKR and modulates its activity. *RNA.* 17:1076–1089. https://doi.org/10.1261/rna.2701111

Li, F., Y. Chen, Z. Zhang, J. Ouyang, Y. Wang, R. Yan, S. Huang, G.F. Gao, G. Guo, and J.L. Chen. 2015. Robust expression of vault RNAs induced by influenza A virus plays a critical role in suppression of PKR-mediated innate immunity. *Nucleic Acids Res.* 43:10321–10337. https://doi.org/10.1093/nar/gkv1078

Li, J.Y., W. Volknandt, A. Dahlstrom, C. Herrmann, J. Blasi, B. Das, and H. Zimmermann. 1999. Axonal transport of ribonucleoprotein particles (vaults). *Neuroscience.* 91:1055–1065. https://doi.org/10.1016/S0306-4522(98)00622-8

Martin, K.C. 2004. Local protein synthesis during axon guidance and synaptic plasticity. *Curr. Opin. Neurobiol.* 14:305–310. https://doi.org/10.1016/j.conb.2004.05.009

Miñones-Moyano, E., M.R. Friedländer, J. Pallares, B. Kagerbauer, S. Porta, G. Escaramís, I. Ferrer, X. Estivill, and E. Martí. 2013. Upregulation of a small vault RNA (svtRNA2-1a) is an early event in Parkinson disease and induces neuronal dysfunction. *RNA Biol.* 10:1093–1106. https://doi.org/10.4161/rna.24813

Mohammad-Rezazadeh, I., J. Frohlich, S.K. Loo, and S.S. Jeste. 2016. Brain connectivity in autism spectrum disorder. *Curr. Opin. Neurol.* 29:137–147. https://doi.org/10.1097/WCO.0000000000000301

Mori, D., M. Yamada, Y. Mimori-Kiyosue, Y. Shirai, A. Suzuki, S. Ohno, H. Saya, A. Wynshaw-Boris, and S. Hirotsune. 2009. An essential role of the aPKC-Aurora A-NDEL1 pathway in neurite elongation by modulation of microtubule dynamics. *Nat. Cell Biol.* 11:1057–1068. https://doi.org/10.1038/ncb1919

Morrison, D.K., and R.J. Davis. 2003. Regulation of MAP kinase signaling modules by scaffold proteins in mammals. *Annu. Rev. Cell Dev. Biol.* 19:91–118. https://doi.org/10.1146/annurev.cellbio.19.111401.091942

Nandy, C., J. Mrázek, H. Stoiber, F.A. Grässer, A. Hüttenhofer, and N. Polacek. 2009. Epstein-barr virus-induced expression of a novel human vault RNA. *J. Mol. Biol.* 388:776–784. https://doi.org/10.1016/j.jmb.2009.03.031

Nikonova, A.S., I. Astsaturov, I.G. Serebriiskii, R.L. Dunbrack Jr., and E.A. Golemis. 2013. Aurora A kinase (AURKA) in normal and pathological cell division. *Cell. Mol. Life Sci.* 70:661–687. https://doi.org/10.1007/s00018-012-1073-7

Numakawa, T., E. Kumamaru, N. Adachi, Y. Yagasaki, A. Izumi, and H. Kunugi. 2009. Glucocorticoid receptor interaction with TrkB promotes BDNF-triggered PLC-gamma signaling for glutamate release via a glutamate transporter. *Proc. Natl. Acad. Sci. USA.* 106:647–652. https://doi.org/10.1073/pnas.0800888106

Ordan, M., C. Pallara, G. Maik-Rachline, T. Hanoch, F.L. Gervasio, F. Glaser, J. Fernandez-Recio, and R. Seger. 2018. Intrinsically active MEK variants are differentially regulated by proteinases and phosphatases. *Sci. Rep.* 8:11830. https://doi.org/10.1038/s41598-018-30202-5

Pan, H.C., J.F. Lin, L.P. Ma, Y.Q. Shen, and M. Schachner. 2013. Major vault protein promotes locomotor recovery and regeneration after spinal cord injury in adult zebrafish. *Eur. J. Neurosci.* 37:203–211. https://doi.org/10.1111/ejn.12038

Paspalas, C.D., C.C. Perley, D.V. Venkitaramani, S.M. Goebel-Goody, Y. Zhang, P. Kurup, J.H. Mattis, and P.J. Lombroso. 2009. Major vault protein is expressed along the nucleus-neurite axis and associates with mRNAs in cortical neurons. *Cereb. Cortex.* 19:1666–1677. https://doi.org/10.1093/cercor/bhn203

Pollarolo, G., J.G. Schulz, S. Munck, and C.G. Dotti. 2011. Cytokinesis remnants define first neuronal asymmetry in vivo. *Nat. Neurosci.* 14:1525–1533. https://doi.org/10.1038/nn.2976

Rangaraju, V., M. Lauterbach, and E.M. Schuman. 2019. Spatially Stable Mitochondrial Compartments Fuel Local Translation during Plasticity. *Cell.* 176:73–84.e15. https://doi.org/10.1016/j.cell.2018.12.013

Richter, J.D., and N. Sonenberg. 2005. Regulation of cap-dependent translation by eIF4E inhibitory proteins. *Nature.* 433:477–480. https://doi.org/10.1038/nature03205

Sabin, L.R., M.J. Delás, and G.J. Hannon. 2013. Dogma derailed: the many influences of RNA on the genome. *Mol. Cell.* 49:783–794. https://doi.org/10.1016/j.molcel.2013.02.010

Seger, R., N.G. Ahn, J. Posada, E.S. Munar, A.M. Jensen, J.A. Cooper, M.H. Cobb, and E.G. Krebs. 1992. Purification and characterization of mitogen-activated protein kinase activator(s) from epidermal growth factor-stimulated A431 cells. *J. Biol. Chem.* 267:14373–14381.

Stadler, P.F., J.J. Chen, J. Hackermüller, S. Hoffmann, F. Horn, P. Khaitovich, A.K. Kretzschmar, A. Mosig, S.J. Prohaska, X. Qi, et al. 2009. Evolution of vault RNAs. *Mol. Biol. Evol.* 26:1975–1991. https://doi.org/10.1093/molbev/msp112

Sweatt, J.D. 2004. Mitogen-activated protein kinases in synaptic plasticity and memory. *Curr. Opin. Neurobiol.* 14:311–317. https://doi.org/10.1016/j.conb.2004.04.001

Thomas, G.M., and R.L. Huganir. 2004. MAPK cascade signalling and synaptic plasticity. *Nat. Rev. Neurosci.* 5:173–183. https://doi.org/10.1038/nrn1346

Tuck, A.C., and D. Tollervey. 2011. RNA in pieces. *Trends Genet.* 27:422–432. https://doi.org/10.1016/j.tig.2011.06.001

van Zon, A., M.H. Mossink, R.J. Scheper, P. Sonneveld, and E.A. Wiemer. 2003a. The vault complex. *Cell. Mol. Life Sci.* 60:1828–1837. https://doi.org/10.1007/s00018-003-3030-y

van Zon, A., M.H. Mossink, M. Schoester, A.B. Houtsmuller, G.L. Scheffer, R.J. Scheper, P. Sonneveld, and E.A. Wiemer. 2003b. The formation of vault-tubes: a dynamic interaction between vaults and vault PARP. *J. Cell Sci.* 116:4391–4400. https://doi.org/10.1242/jcs.00749

Wakatsuki, S., A. Furuno, M. Ohshima, and T. Araki. 2015. Oxidative stress-dependent phosphorylation activates ZNRF1 to induce neuronal/axonal degeneration. *J. Cell Biol.* 211:881–896. https://doi.org/10.1083/jcb.201506102

Wakatsuki, S., F. Saitoh, and T. Araki. 2011. ZNRF1 promotes Wallerian degeneration by degrading AKT to induce GSK3B-dependent CRMP2 phosphorylation. *Nat. Cell Biol.* 13:1415–1423. https://doi.org/10.1038/ncb2373

Wakatsuki, S., S. Tokunaga, M. Shibata, and T. Araki. 2017. GSK3B-mediated phosphorylation of MCL1 regulates axonal autophagy to promote

Wallerian degeneration. *J. Cell Biol.* 216:477–493. https://doi.org/10.1083/jcb.201606020

Wassarman, K.M., and G. Storz. 2000. 6S RNA regulates E. coli RNA polymerase activity. *Cell.* 101:613–623. https://doi.org/10.1016/S0092-8674(00)80873-9

Yagasaki, Y., T. Numakawa, E. Kumamaru, T. Hayashi, T.P. Su, and H. Kunugi. 2006. Chronic antidepressants potentiate via sigma-1 receptors the brain-derived neurotrophic factor-induced signaling for glutamate release. *J. Biol. Chem.* 281:12941–12949. https://doi.org/10.1074/jbc.M508157200

Yao, J., A. Nowack, P. Kensel-Hammes, R.G. Gardner, and S.M. Bajjalieh. 2010. Cotrafficking of SV2 and synaptotagmin at the synapse. *J. Neurosci.* 30:5569–5578. https://doi.org/10.1523/JNEUROSCI.4781-09.2010

Yogev, S., and K. Shen. 2017. Establishing Neuronal Polarity with Environmental and Intrinsic Mechanisms. *Neuron.* 96:638–650. https://doi.org/10.1016/j.neuron.2017.10.021

Yuan, J., W.H. Ng, Z. Tian, J. Yap, M. Baccarini, Z. Chen, and J. Hu. 2018. Activating mutations in MEK1 enhance homodimerization and promote tumorigenesis. *Sci. Signal.* 11:eaar6795. https://doi.org/10.1126/scisignal.aar6795
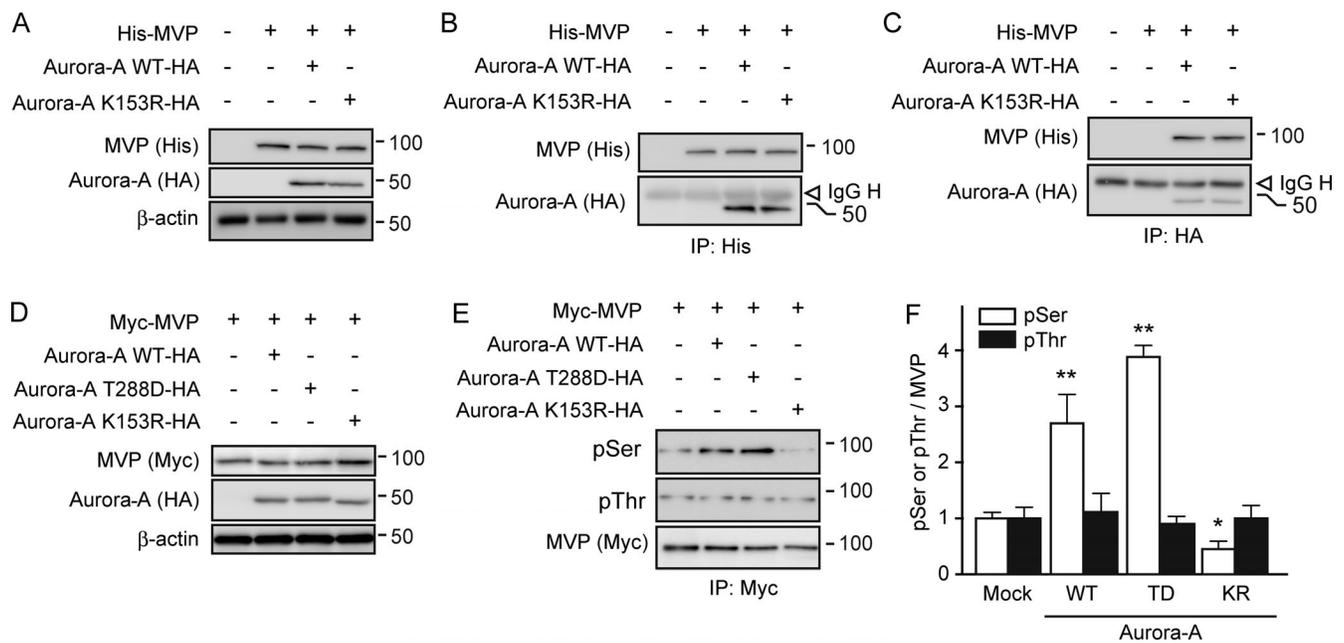
Supplemental material

Figure S1. **Aurora-A interacts with MVP in Neuro2-a cells. (A–C)** MVP is associated with Aurora-A irrespective of its kinase activity. Lysates were prepared from Neuro-2a cells overexpressing HA-tagged WT Aurora-A or Aurora-A K153R mutant with His-tagged MVP. Representative immunoblots (A) and immunoprecipitations using the indicated antibodies (B and C) analyzed by immunoblotting are shown. β-Actin serves as a loading control. **(D–F)** Aurora-A phosphorylates MVP on serine residues. Lysates were prepared from Neuro-2a cells overexpressing HA-tagged WT or the indicated mutant forms of Aurora-A together with Myc-tagged MVP. Representative immunoblots (D) and immunoprecipitations using a Myc antibody (E) analyzed by immunoblotting are shown. β-Actin serves as a loading control. Quantified expression levels for phosphorylated MVP normalized to β-actin relative to the mock-transfected control (mean ± SEM, n = 5) are shown in F. Significant differences from the control (*, $P < 0.05$; **, $P < 0.01$) were determined by one-way ANOVA with Tukey's post hoc test. pSer, phospho-serine; pThr, phospho-threonine; IgG H, IgG heavy chain; IP, immunoprecipitation.
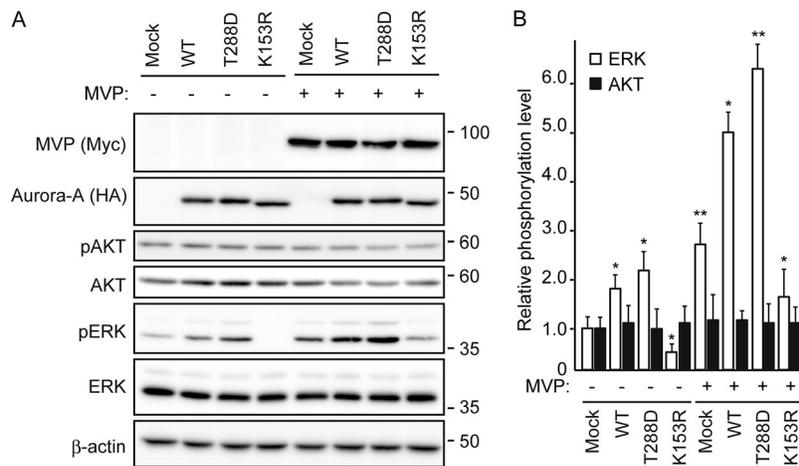
Figure S2. **Aurora-A in concert with MVP enhances ERK signaling in Neuro2-a cells.** Lysates were prepared from Neuro2-a cells overexpressing HA-tagged Aurora-A WT, Aurora-A T288D, or Aurora-A K153R, together with/without Myc-tagged MVP. **(A)** Representative immunoblots for the expression of the indicated molecules. β-Actin serves as a loading control. **(B and C)** Phosphorylation levels of ERK (B) and AKT (C; calculated as phosphorylated ERK/total ERK and phosphorylated AKT/total AKT, respectively, normalized to the value in mock-translated control without MVP expression) are shown for each treatment. Significant differences from the control (mock; *, P < 0.05; **, P < 0.01) were determined by one-way ANOVA with Tukey's post hoc test.
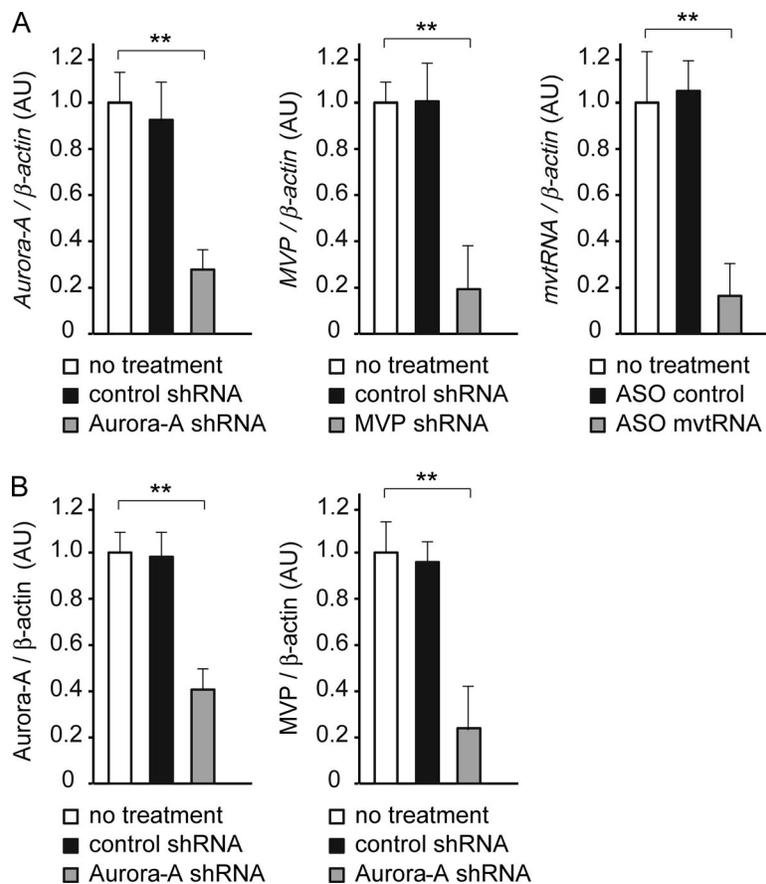

Figure S3. **Down-regulation of the indicated genes by the specific shRNA or ASO in cultured cortical neurons.** The shRNA-mediated down-regulation of the indicated genes was performed in cultured cortical neurons via lentivirus vectors or ASO. **(A and B)** The down-regulation of each molecule was confirmed by quantitative RT-PCR (A) and immunoblot analysis (B). The expression levels of each molecule normalized to β-actin are shown relative to that of the no-treatment control. Data are presented as the mean ± SEM (n = 5). Significant differences from the control (**, P < 0.01) were determined by one-way ANOVA with Tukey's post hoc test. AU, arbitrary units.
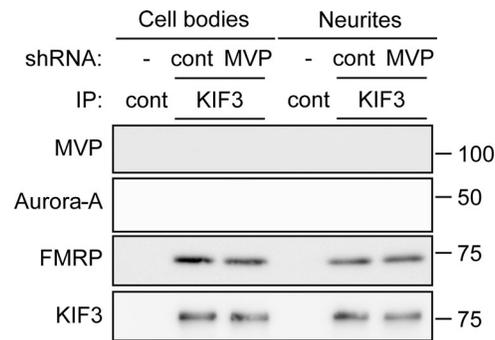
Figure S4. **No interaction of KIF3 with the MVP–Aurora-A complex was detected in cultured cortical neurons.** The molecular interaction between KIF3 and the MVP–Aurora-A complex was assessed by coimmunoprecipitation experiments using an anti-KIF3 antibody in lysates from neurites. Representative immunoblots and immunoprecipitation (IP) analyzed by immunoblotting with the indicated antibodies. FMRP serves as positive control for interaction with KIF3. Note that FMRP, but neither MVP nor Aurora-A, interacts with KIF3. Cont, control.